

RIS-assisted Millimeter-Wave MIMO Communication Systems: Ergodic Capacity Analysis and Optimization

Renwang Li, Shu Sun, Yuhang Chen, Chong Han, Meixia Tao, *Fellow, IEEE*

Abstract

Reconfigurable intelligent surfaces (RISs) have emerged as a prospective technology for next-generation wireless networks due to their potential in coverage and capacity enhancement. The analysis and optimization of ergodic capacity for RIS-assisted communication systems have been investigated extensively. However, the Rayleigh or Rician channel model is usually utilized in the existing work, which is not suitable for millimeter-wave (mmWave) multiple-input multiple-output (MIMO) systems. Thus, we fill the gap and consider the ergodic capacity of RIS-assisted mmWave MIMO communication systems under the Saleh-Valenzuela channel model. Firstly, we derive tight approximations of ergodic capacity and a tight upper bound in high signal-to-noise ratio regime. Then, we aim to maximize the ergodic capacity by jointly designing the transmit covariance matrix at the base station and the reflection coefficients at the RIS. Specifically, the transmit covariance matrix is optimized by the water-filling algorithm and the reflection coefficients are optimized using the Riemannian conjugate gradient algorithm. Simulation results validate the tightness of the derived ergodic capacity approximations and the effectiveness of the proposed algorithms.

Index Terms

R. Li, S. Sun, and M. Tao are with Department of Electronic Engineering, Shanghai Jiao Tong University, Shanghai, China (emails:{renwanglee, shusun, mxtao}@sjtu.edu.cn).

Y. Chen is with Terahertz Wireless Communications (TWC) Laboratory, Shanghai Jiao Tong University, Shanghai, China (emails:{yuhang.chen}@sjtu.edu.cn).

C. Han is with Terahertz Wireless Communications (TWC) Laboratory and Department of Electronic Engineering, Shanghai Jiao Tong University, Shanghai, China (emails:{chong.han}@sjtu.edu.cn).

Reconfigurable intelligent surface, ergodic capacity, statistical channel state information (CSI), transmit covariance matrix, reflection coefficients, millimeter-wave communications.

I. INTRODUCTION

The millimeter-wave (mmWave) communication over the 30-300 GHz spectrum is regarded as a promising technology for 5G and beyond wireless networks due to its large bandwidth and the potential to offer high communication data rates [1], [2]. Large antenna arrays are usually adopted in mmWave communications since they can form highly directional beams to compensate for the severe path loss compared with sub-6 GHz. Meanwhile, the high directivity makes mmWave communication much more sensitive to signal blockage, which can be frequent in the environment [3].

To overcome the blockage issue, reconfigurable intelligent surface (RIS) has been recently introduced to enlarge the coverage of the mmWave communication systems [4], [5]. Specifically, RIS is an artificial meta-surface that is composed of a large number of nearly passive units and can be controlled efficiently by a smart controller [6]. RIS can smartly reflect the signals from the base station (BS) to multiple users by adjusting the amplitude and phase of the incident signals. When the BS-user channel is blocked, RIS can create a virtual BS-RIS-user channel, and thus improve the coverage of mmWave systems. There are often no radio frequency (RF) components on RIS. Therefore, RIS is an efficient and cost-effective solution for the blockage problem in mmWave systems.

Motivated by the above attractive advantages, RIS-aided communication systems have been widely studied in various scenarios, e.g., [7]–[11]. The authors in [7] consider the power minimization problem for an RIS-assisted multiple-input single-output (MISO) downlink multi-user system subject to signal-to-interference-plus-noise ratio (SINR) constraints. The weighted sum-rate is maximized in [8] under the maximum power budget. The authors of [9] focus on maximizing the secrecy rate of the legitimate user. The authors in [10] aim to maximize the capacity of an RIS-aided multiple-input multiple-output (MIMO) system and propose an alternating optimization based algorithm. Pertaining to mmWave MIMO systems, the channel capacity maximization problem is investigated in [11] by exploiting the sparse structure of mmWave channel to propose an efficient manifold-based algorithm.

However, all of the above contributions are based on instantaneous channel state information

(CSI), which is very challenging to obtain due to the fact that RIS is a passive component and can not sense the environment independently [4], [6]. Thus, some researchers attempt to explore the statistical CSI in RIS-aided communication systems [12]–[19]. For single-input single-output systems, [12] considers the Rayleigh fading channel and computes the closed-form expression of the coverage probability and the upper bound of ergodic capacity, while the Rician channel is considered in [13]. For MISO systems, [14] derives a tight upper bound of the ergodic capacity under Rician fading channels. The maximum ratio transmitting is adopted at the BS and an optimal reflection coefficients design at the RIS is proposed based on the upper bound. In [15], the authors take the active beamforming at the BS into consideration when deriving the ergodic capacity. Both [14] and [15] consider single user scenario, which is extended to the multiuser case in [16]. For MIMO systems, [17] considers single-stream transmission and obtains a tight upper bound of the ergodic capacity under the Rician channels, while the multi-stream transmission case is considered in [18]. In addition, the lower and upper bounds of the ergodic capacity are derived in [19] when equal power allocation is adopted at the BS. Note that all these works consider the Rayleigh or Rician channels. However, the Rayleigh or Rician channels are not suitable for mmWave systems due to the limited scattering, which is usually characterized by the Saleh-Valenzuela (SV) channel [11], [20]–[24]. Therefore, we aim to fill the gap in this work inspired by [24]. To the best of the authors' knowledge, this is the first effort to derive the ergodic capacity under the SV channel in RIS-aided mmWave MIMO communication systems.

Against the above background, we concentrate on an RIS-aided downlink mmWave MIMO communication systems with the statistical CSI and SV channel model. The main contributions of this study are summarized as follows:

- We derive a tight closed-form ergodic capacity approximation for the RIS-aided mmWave MIMO communication systems based on the majorization theory and Jensen's inequality. The approximation holds for arbitrary numbers of paths, antennas and reflection units, and arbitrary antenna structures.
- We derive a tight upper bound of the ergodic capacity in high-SNR regime. The upper bound shows that the ergodic capacity increases logarithmically with the signal-to-noise ratio (SNR), the number of antennas at the BS and user, the number of the reflection units at the RIS, and the eigenvalues of the steering matrices associated with the BS, user and RIS.

- We maximize the ergodic capacity by jointly designing the transmit covariance matrix at the BS and the reflection coefficients at the RIS based on the derived closed-form approximation. Specifically, the transmit covariance matrix is optimized by the water-filling algorithm and the reflection coefficients are optimized by the Riemannian conjugate gradient (RCG) algorithm.

Finally, we conduct comprehensive simulations and validate the tightness of the derived ergodic capacity approximation. It is shown that the ergodic capacity after optimization could be improved by about 20 bits/s/Hz. In addition, when the BS allocates equal power over transmit signals, the ergodic capacity remains unchanged after the number of antennas at the BS reaches a certain amount. Furthermore, if we are allowed to optimize only one variable of the transmit covariance matrix and the reflection coefficients, optimizing the reflection coefficients is more effective than optimizing the transmit covariance matrix only in the case of a large number of reflection units. Thanks to the low-cost passive elements, RIS usually has a large number of reflection units. In this case, the system still performs well if the BS allocates equal power and the reflection coefficients at the RIS are optimized.

The rest of the paper is organized as follows. Section II introduces the system model and the problem formulation. Section III adopts the majorization theory to derive the ergodic capacity approximation and the upper bound in high-SNR regime. Section IV designs the transmit covariance matrix and the reflection coefficients. Section V presents the extensive simulation results and Section VI concludes this paper.

Notations: The imaginary unit is denoted by $j = \sqrt{-1}$. Vectors and matrices are denoted by bold-face lower-case and upper-case letters, respectively. $\mathbb{C}^{x \times y}$ denotes the space of $x \times y$ complex-valued matrices. \mathbf{x}^* , \mathbf{x}^T , and \mathbf{x}^H denote the conjugate, transpose and conjugate transpose of vector \mathbf{x} . \mathbf{I} denotes an identity matrix of appropriate dimensions. \odot denotes the Hadamard product. $\mathbb{E}(\cdot)$ denotes the stochastic expectation. $\Re(\cdot)$ denote the real part of a complex number. The $\text{tr}(\cdot)$, $\det(\cdot)$ and $\text{rank}(\cdot)$ denote the trace, determinant and rank operation, respectively. $\text{diag}(\mathbf{x})$ denotes a diagonal matrix with each diagonal element being the corresponding element in \mathbf{x} . $\nabla f(\mathbf{x}_i)$ denotes the gradient vector of function $f(\mathbf{x})$ at the point \mathbf{x}_i . The distribution of a circularly symmetric complex Gaussian random vector with mean vector x and covariance matrix Σ is denoted by $\mathcal{CN}(x, \Sigma)$; and \sim stands for “distributed as”. The exponential random variable X with parameter λ is given by $X \sim \exp(\lambda)$.

II. SYSTEM MODEL AND PROBLEM FORMULATION

A. System Model

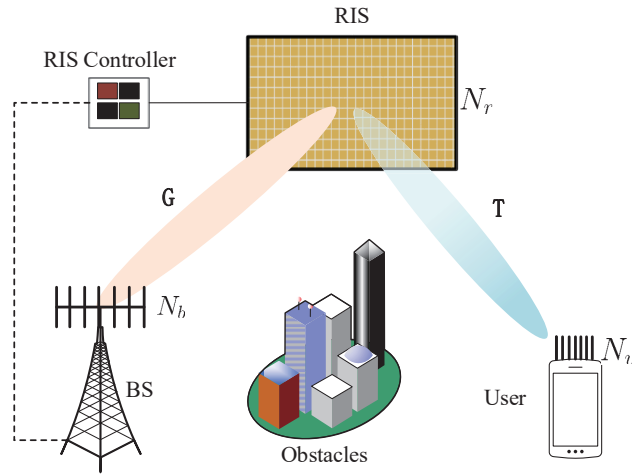


Fig. 1: Illustration of an RIS-aided mmWave MIMO system.

As shown in Fig. 1, we consider an RIS-aided downlink mmWave MIMO communication system, where one BS equipped with $N_b \geq 1$ antennas communicates with a user equipped with $N_u \geq 1$ antennas, via the assistance of one RIS equipped with $N_r \geq 1$ nearly passive reflecting units. We assume that the BS-user direct link is blocked due to unfavorable propagation conditions. $\mathbf{G} \in \mathbb{C}^{N_r \times N_b}$ and $\mathbf{T} \in \mathbb{C}^{N_u \times N_r}$ denote the channel matrix from BS to RIS, and from RIS to user, respectively, and $\mathbf{s} \in \mathbb{C}^{N_b \times 1}$ denotes the zero-mean transmitted Gaussian vector with covariance matrix $\mathbf{Q} \in \mathbb{C}^{N_b \times N_b}$. The transmit power constraint at the BS can be expressed as

$$\text{tr} \mathbb{E}\{\mathbf{s}\mathbf{s}^H\} = \text{tr}(\mathbf{Q}) \leq P_T, \quad (1)$$

where $P_T > 0$ is the power budget at the BS. Then, the received vector $\mathbf{y} \in \mathbb{C}^{N_u \times 1}$ at the user can be represented as

$$\mathbf{y} = \mathbf{T}\Theta\mathbf{G}\mathbf{s} + \mathbf{n}, \quad (2)$$

where $\Theta = \text{diag}\{\xi_1 e^{j\theta_1}, \xi_2 e^{j\theta_2}, \dots, \xi_{N_r} e^{j\theta_{N_r}}\}$ represents the response matrix of the RIS, $\theta_i \in [0, 2\pi)$ and $\xi_i \in [0, 1]$ represent the phase shift and the amplitude reflection coefficient of the i -th reflecting unit, respectively, and $\mathbf{n} \sim \mathcal{CN}(\mathbf{0}, \sigma^2 \mathbf{I}_{N_u})$ represents the additive white Gaussian noise with zero mean and variance σ^2 . In this paper, we assume $\xi_i = 1, i = 1, 2, \dots, N_r$ to maximize the signal reflection.

We adopt the widely used narrowband SV channel model for mmWave communications. Suppose uniform linear arrays (ULAs)¹ are equipped at the BS and the user, and a uniform planar array (UPA) is equipped at the RIS. Hence, the narrowband BS-RIS channel \mathbf{G} and RIS-user channel \mathbf{T} can be expressed as

$$\mathbf{G} = \sqrt{\frac{N_r N_b}{P}} \sum_{i=1}^P g_i \mathbf{a}_r(\phi_{r,i}^1, \phi_{r,i}^2) \mathbf{a}_b^H(\phi_{b,i}), \quad (3)$$

$$\mathbf{T} = \sqrt{\frac{N_r N_u}{L}} \sum_{i=1}^L t_i \mathbf{a}_u(\psi_{u,i}) \mathbf{a}_r^H(\psi_{r,i}^1, \psi_{r,i}^2), \quad (4)$$

where $P(L)$ is the number of paths between the BS and the RIS (the RIS and the user), $g_i \sim \mathcal{CN}(0, 1)$ ($t_i \sim \mathcal{CN}(0, 1)$)² denotes complex channel gain of the i -th path, $\phi_{r,i}^1$ ($\psi_{r,i}^1$) and $\phi_{r,i}^2$ ($\psi_{r,i}^2$) denote the azimuth and elevation angles of arrival (departure) associated with the RIS, $\phi_{b,i}$ denotes the angle of departure (AOD) associated with the BS, $\psi_{u,i}$ denotes the angle of arrival (AOA) associated with the user, and $\mathbf{a}_i, i \in \{b, r, u\}$ denote the normalized array response vectors. When an N -antenna ULA is employed, the array response vector is given by

$$\mathbf{a}(\phi) = \frac{1}{\sqrt{N}} \left[1, e^{j\frac{2\pi d}{\lambda} \sin(\phi)}, \dots, e^{j\frac{2\pi d}{\lambda} (N-1) \sin(\phi)} \right]^T, \quad (5)$$

where λ is the signal wavelength, d is the antenna spacing which is assumed to be half wavelength, and ϕ denotes the AOA or AOD. For a UPA with $M = M_y \times M_z$ elements, the array response vector is given by

$$\mathbf{a}(\phi^1, \phi^2) = \frac{1}{\sqrt{M}} \left[1, \dots, e^{j\frac{2\pi d}{\lambda} (m_y \sin \phi^1 \sin \phi^2 + m_z \cos \phi^2)}, \dots, e^{j\frac{2\pi d}{\lambda} ((M_y-1) \sin \phi^1 \sin \phi^2 + (M_z-1) \cos \phi^2)} \right]^T, \quad (6)$$

where d is the unit cell spacing which is assumed to be half wavelength, while ϕ^1 and ϕ^2 denote the azimuth and elevation angles, respectively. Defining $\mathbf{A}_{rp} = [\mathbf{a}_r(\phi_{r,1}^1, \phi_{r,1}^2), \dots, \mathbf{a}_r(\phi_{r,P}^1, \phi_{r,P}^2)] \in \mathbb{C}^{N_r \times P}$, $\mathbf{A}_b = [\mathbf{a}_b(\phi_{b,1}), \mathbf{a}_b(\phi_{b,2}), \dots, \mathbf{a}_b(\phi_{b,P})] \in \mathbb{C}^{N_b \times P}$, $\mathbf{G}_p = \sqrt{\frac{N_r N_b}{P}} \text{diag}(g_1, g_2, \dots, g_P)$, the channel matrix \mathbf{G} (3) can be rewritten as

$$\mathbf{G} = \mathbf{A}_{rp} \mathbf{G}_p \mathbf{A}_b^H. \quad (7)$$

¹We assume the deployment of ULA for ease of exposition. The results can be extended straightforwardly to other antenna topologies, such as, UPA and so on.

²In mmWave MIMO communication systems, it is reasonable to assume that the complex gains of different paths experience the same variances [20]–[22]. Furthermore, the results are extendible to the case of different variances.

Defining $\mathbf{A}_{rL} = [\mathbf{a}_r(\psi_{r,1}^1, \psi_{r,1}^2), \dots, \mathbf{a}_r(\psi_{r,L}^1, \psi_{r,L}^2)] \in \mathbb{C}^{N_r \times L}$, $\mathbf{A}_u = [\mathbf{a}_u(\psi_{b,1}), \dots, \mathbf{a}_u(\psi_{b,L})] \in \mathbb{C}^{N_u \times L}$, $\mathbf{T}_L = \sqrt{\frac{N_r N_u}{L}} \text{diag}(t_1, t_2, \dots, t_L)$, the channel matrix \mathbf{T} (4) can be rewritten as

$$\mathbf{T} = \mathbf{A}_u \mathbf{T}_L \mathbf{A}_{rL}^H. \quad (8)$$

Assume that the instantaneous CSI is unknown, the ergodic capacity of the RIS-aided mmWave MIMO communication systems can be expressed as

$$C(\mathbf{Q}, \Theta) = \max_{\text{Tr}(\mathbf{Q}) \leq P_T} \mathbb{E}_{\mathbf{H}} \left[\log_2 \det \left(\mathbf{I}_{N_u} + \frac{1}{\sigma^2} \mathbf{H} \mathbf{Q} \mathbf{H}^H \right) \right], \quad (9)$$

where $\mathbf{H} = \mathbf{T} \Theta \mathbf{G}$ denotes the BS-RIS-user channel.

B. Problem Formulation

We aim to maximize the ergodic capacity by jointly optimizing the transmit covariance matrix at the BS and the reflection coefficients at the RIS, subject to the maximum power budget (1) at the BS. Therefore, the problem can be formulated as

$$\mathcal{P}_0 : \max_{\mathbf{Q}, \Theta} C(\mathbf{Q}, \Theta) \quad (10a)$$

$$\text{s.t.} \quad \text{tr}(\mathbf{Q}) \leq P_T, \quad (10b)$$

$$\mathbf{Q} \succeq 0, \quad (10c)$$

$$\Theta = \text{diag}(e^{j\theta_1}, e^{j\theta_2}, \dots, e^{j\theta_{N_r}}). \quad (10d)$$

The problem \mathcal{P}_0 is very challenging mainly due to two facts. To begin with, there is no explicit expression of the ergodic capacity, which prevents further optimization exploration. Secondly, the problem is highly non-convex due to the unit-modulus phase shifts constraints (10d), and thus difficult to be optimally solved. In the following, we will first find the explicit expression to approximate the ergodic capacity, and then maximize the ergodic capacity by optimizing \mathbf{Q} and Θ .

III. THE ERGODIC CAPACITY

In this section, we first derive the ergodic capacity approximation as well as the high-SNR capacity upper bound according to the majorization theory. Then, explicit expression is obtained via the Jensen's inequality.

A. Approximation of the Ergodic Capacity

Theorem 1: Under the narrowband SV channel model expressed in (7) and (8), the ergodic capacity of the RIS-aided mmWave MIMO communication systems can be approximated by

$$C_{app} = \mathbb{E}_{g,t} \left[\sum_{i=1}^{N_s} \log_2 \left(1 + \frac{N_b N_u N_r^2}{\sigma^2 P L} d_{b,i} d_{u,i} d_{r,i} |g_i|^2 |t_i|^2 \right) \right], \quad (11)$$

where $N_s = \min(\text{rank}(\mathbf{A}_b^H \mathbf{Q} \mathbf{A}_b), \text{rank}(\mathbf{A}_u^H \mathbf{A}_u), \text{rank}(\mathbf{X}^H \mathbf{X}))$, $\mathbf{X} = \mathbf{A}_{rL}^H \mathbf{\Theta} \mathbf{A}_{rp}$, and $(d_{b,1}, \dots, d_{b,N_s})$, $(d_{u,1}, d_{u,2}, \dots, d_{u,N_s})$ and $(d_{r,1}, d_{r,2}, \dots, d_{r,N_s})$ are descending ordered eigenvalues of $\mathbf{A}_b^H \mathbf{Q} \mathbf{A}_b$, $\mathbf{A}_u^H \mathbf{A}_u$ and $\mathbf{X}^H \mathbf{X}$, respectively.

Proof: See Appendix A. ■

It is found that the ergodic capacity is closely related to the eigenvalues of the matrices associated with the BS, the user and the RIS. Their influences on the ergodic capacity can be clearly seen from $\mathbf{A}_b^H \mathbf{Q} \mathbf{A}_b$, $\mathbf{A}_u^H \mathbf{A}_u$ and $\mathbf{X}^H \mathbf{X}$.

Proposition 1: When \mathbf{A}_b , \mathbf{A}_u , \mathbf{A}_{rp} and \mathbf{A}_{rL} are composed of the columns of unitary matrices, e.g., the discrete Fourier matrices, and the AOA at the RIS is symmetric to the AOD at the RIS, i.e., $\phi_{r,i}^1 = \psi_{r,i}^1$, $\phi_{r,i}^2 = \psi_{r,i}^2$, $\forall i$, $\mathbf{Q} = \frac{P_r}{N_b} \mathbf{I}_{N_b}$, and $\mathbf{\Theta} = \mathbf{I}_{N_r}$, the derived ergodic capacity approximation C_{app} is identical to the exact ergodic capacity, i.e.,

$$C_{app} = C_{exact}. \quad (12)$$

Proof: See Appendix B. ■

Proposition 1 implies that the derived capacity approximation exhibits tight performance when the BS allocates equal power, the RIS acts like a mirror, and all steering response matrices are taken from columns of unitary matrices. Specifically, when the number of the antennas or the reflection units is very large, the steering response matrices become asymptotically semi-unitary.

Considering the typical scenario with line-of-sight paths to and from the RIS and the beamforming technique with large antenna arrays, the RIS-aided mmWave systems are likely to operate in high-SNR regime. The following proposition exploits the upper bound of the ergodic capacity in high-SNR regime.

Proposition 2: Under the narrowband SV channel model, the ergodic capacity of the RIS-aided mmWave MIMO communication systems in high-SNR regime can be upper bounded by

$$C_h \leq C_h^{upper} = \sum_{i=1}^{N_s} \frac{1}{\ln 2} \left(-2\gamma + \ln \left(\frac{N_b N_u N_r^2}{\sigma^2 P L} d_{b,i} d_{u,i} d_{r,i} \right) \right), \quad (13)$$

where C_h denotes the ergodic capacity in the high-SNR regime, $\gamma \approx 0.5772$ is the Euler-Mascheroni constant, $(d_{b,1}, d_{b,2}, \dots, d_{b,N_s})$, $(d_{u,1}, d_{u,2}, \dots, d_{u,N_s})$ and $(d_{r,1}, d_{r,2}, \dots, d_{r,N_s})$ are descending ordered eigenvalues of $\mathbf{A}_b^H \mathbf{Q} \mathbf{A}_b$, $\mathbf{A}_u^H \mathbf{A}_u$ and $\mathbf{X}^H \mathbf{X}$, respectively. The equality holds when $N_s = P = L$.

Proof: See Appendix C. ■

In order to exploit the relationship between the upper bound and the SNR, we transform the upper bound to another formulation. Let $\mathbf{Q} = P_T \tilde{\mathbf{Q}}$ and $\mathbf{A}_b^H \tilde{\mathbf{Q}} \mathbf{A}_b = \mathbf{U}_b^H \tilde{\mathbf{D}}_b \mathbf{U}_b$, where $\tilde{\mathbf{D}}_b = \text{diag}(\tilde{d}_{b,1}, \tilde{d}_{b,2}, \dots, \tilde{d}_{b,P})$ is composed of the eigenvalues of $\mathbf{A}_b^H \tilde{\mathbf{Q}} \mathbf{A}_b$ in descending order. Therefore, the upper bound C_h^{upper} can be transformed to

$$C_h \leq C_h^{upper} = \sum_{i=1}^{N_s} \frac{1}{\ln 2} \left(-2\gamma + \ln \left(\frac{P_T N_b N_u N_r^2}{\sigma^2 PL} \tilde{d}_{b,i} d_{u,i} d_{r,i} \right) \right). \quad (14)$$

It can be found that when the SNR is large, the upper bound of the ergodic capacity increases logarithmically with SNR, N_b , N_u , N_r ³ and the eigenvalues of the matrices $\mathbf{A}_b^H \tilde{\mathbf{Q}} \mathbf{A}_b$, $\mathbf{A}_u^H \mathbf{A}_u$ and $\mathbf{X}^H \mathbf{X}$. Specifically, the upper bound of the ergodic capacity has no relationship with the number of antennas at the BS when the number of antennas exceeds a certain amount and the BS allocates equal power over transmit signals, i.e., $\tilde{\mathbf{Q}} = \frac{1}{N_b} \mathbf{I}_{N_b}$. It is because of the asymptotic orthogonality of the array response vectors when the number of antennas is large and $\{\tilde{d}_{b,i}\}_{\forall i}$ is nearly equal to one.

Theorem 2: The ergodic capacity of the RIS-aided mmWave MIMO communication systems can be further approximated by

$$C_{app} = \frac{1}{\ln 2} \sum_{i=1}^{N_s} \int_0^\infty e^{-z} e^{\frac{1}{\alpha_i z}} E_1 \left(\frac{1}{\alpha_i z} \right) dz, \quad (15)$$

where $\alpha_i = \frac{N_b N_u N_r^2}{\sigma^2 PL} d_{b,i} d_{u,i} d_{r,i}$, and $E_1(z)$ is the exponential integral function, which is defined as $E_1(z) = \int_1^\infty x^{-1} e^{-zx} dx$, $z > 0$.

Proof: See Appendix D. ■

Although Theorem 2 gives an explicit expression of the ergodic capacity, there are complex integral items involved in the expression (15), which is difficult for further optimization.

³We only consider far-field scenario in this work.

B. Jensen's Approximations for the Ergodic Capacity

It is difficult to utilize the expression (15) in the optimization procedure. Therefore, we further simplify the expression of the ergodic capacity via the Jensen's inequality.

Proposition 3: Under the narrowband SV channel model, the ergodic capacity of the RIS-aided mmWave MIMO communication systems can be approximated by

$$C_{Jen1} = \sum_{i=1}^{N_s} \log_2 \left(1 + \frac{N_b N_u N_r^2}{\sigma^2 P L} d_{b,i} d_{u,i} d_{r,i} \right). \quad (16)$$

Proof: According to the Jensen's inequality $\mathbb{E}\{\log_2(1+x)\} \leq \log_2(1+\mathbb{E}\{x\})$ for $x \geq 0$, we have

$$\begin{aligned} C_{app} &= \mathbb{E}_{g,t} \left[\sum_{i=1}^{N_s} \log_2 \left(1 + \frac{N_b N_u N_r^2}{\sigma^2 P L} d_{b,i} d_{u,i} d_{r,i} |g_i|^2 |t_i|^2 \right) \right] \\ &\leq \sum_{i=1}^{N_s} \log_2 \left(1 + \mathbb{E} \left\{ \frac{N_b N_u N_r^2}{\sigma^2 P L} d_{b,i} d_{u,i} d_{r,i} |g_i|^2 |t_i|^2 \right\} \right) \\ &= C_{Jen1}. \end{aligned} \quad (17)$$

Since $|g_i|^2 \sim \exp(1)$, $|t_i|^2 \sim \exp(1)$, and $|g_i|^2$ and $|t_i|^2$ are independent with each other, we have

$$\mathbb{E} \left\{ \frac{N_b N_u N_r^2}{\sigma^2 P L} d_{b,i} d_{u,i} d_{r,i} |g_i|^2 |t_i|^2 \right\} = \frac{N_b N_u N_r^2}{\sigma^2 P L} d_{b,i} d_{u,i} d_{r,i} \mathbb{E}\{|g_i|^2\} \mathbb{E}\{|t_i|^2\} = \frac{N_b N_u N_r^2}{\sigma^2 P L} d_{b,i} d_{u,i} d_{r,i}. \quad (18)$$

Substituting (18) to (17), we can obtain (16). \blacksquare

It is important to find that the Jensen's approximation C_{Jen1} (16) is very succinct, which only contains the product of the eigenvalues and the summation over data streams. We can find that the ergodic capacity of the RIS-aided mmWave MIMO system increases logarithmically with the number of antennas of the BS and the user, the number of the reflection units of the RIS, and the eigenvalues of the matrices $\mathbf{A}_b^H \mathbf{Q} \mathbf{A}_b$, $\mathbf{A}_u^H \mathbf{A}_u$ and $\mathbf{X}^H \mathbf{X}$. However, the approximation C_{Jen1} is loose, which can be found in the simulation section.

In order to find tighter approximation, we need to consider the order statistic. According to [[25], Theorem 1], let a_1, a_2, \dots, a_n and b_1, b_2, \dots, b_n be positive real numbers with $0 \leq a_1 \leq a_2 \leq \dots \leq a_n$ and $0 \leq b_1 \leq b_2 \leq \dots \leq b_n$, then

$$\prod_{k=1}^n (1 + a_k b_k) \geq \prod_{k=1}^n (1 + a_k b_{\theta(k)}) \geq \prod_{k=1}^n (1 + a_k b_{n-k+1}), \quad (19)$$

where θ is a permutation of $\{1, 2, \dots, n\}$.

The expressions (15) and (16) are actually obtained when $\{|g_i|^2\}$ and $\{|t_i|^2\}$ are not ordered, and the Jensen's approximation C_{Jen1} is a little larger than the actual results. Therefore, we can obtain tighter approximation if $\{|g_i|^2\}$ and $\{|t_i|^2\}$ are ascending ordered sequences since $\{d_{b,i}d_{u,i}d_{r,i}\}$ are descending ordered sequences. Specifically, we have the following proposition.

Proposition 4: Under the narrowband SV channel model, the ergodic capacity of the RIS-aided mmWave MIMO communication systems can be approximated by

$$C_{Jen2} = \sum_{i=1}^{N_s} \log_2 \left(1 + \sum_{j=1}^i \frac{1}{P-j+1} \sum_{j=1}^i \frac{1}{L-j+1} \frac{N_b N_u N_r^2}{\sigma^2 P L} d_{b,i} d_{u,i} d_{r,i} \right). \quad (20)$$

Proof: Let $\{|g_{(i)}|^2\}$ and $\{|t_{(i)}|^2\}$ denote the ascending ordered sequences of $\{|g_i|^2\}$ and $\{|t_i|^2\}$, respectively. According to the order statistic results [[26], Eq. (11.2)], the expectation of $|g_{(i)}|^2$ and $|t_{(i)}|^2$ can be calculated as

$$\begin{aligned} \mathbb{E}\{|g_{(i)}|^2\} &= \sum_{j=1}^i \frac{1}{P-j+1}, \\ \mathbb{E}\{|t_{(i)}|^2\} &= \sum_{j=1}^i \frac{1}{L-j+1}. \end{aligned} \quad (21)$$

Then, according to the Jensen's inequality, we have

$$\begin{aligned} C_{app} &= \mathbb{E}_{g,t} \left[\sum_{i=1}^{N_s} \log_2 \left(1 + \frac{N_b N_u N_r^2}{\sigma^2 P L} d_{b,i} d_{u,i} d_{r,i} |g_{(i)}|^2 |t_{(i)}|^2 \right) \right] \\ &\leq \sum_{i=1}^{N_s} \log_2 \left(1 + \frac{N_b N_u N_r^2}{\sigma^2 P L} d_{b,i} d_{u,i} d_{r,i} \mathbb{E}\{|g_{(i)}|^2 |t_{(i)}|^2\} \right) \\ &= C_{Jen2}. \end{aligned} \quad (22)$$

■

Note that both C_{Jen1} and C_{Jen2} have the concise form of the approximation of the ergodic capacity. However, C_{Jen2} exhibits tighter approximation because it exploits the order statistic, and the Jensen's upper bound is minimized by multiplying $d_{b,i}d_{u,i}d_{r,i}$ and $\mathbb{E}\{|g_{(i)}|^2 |t_{(i)}|^2\}$ in opposite order. Consequently, we adopt the expression C_{Jen2} (20) to approximate the ergodic capacity in the following.

IV. TRANSMIT COVARIANCE MATRIX AND REFLECTION COEFFICIENTS OPTIMIZATION

With the obtained approximate expression C_{Jen2} of the ergodic capacity of the RIS-aided mmWave MIMO communication system, we now focus on maximizing C_{Jen2} by jointly opti-

mizing the transmit covariance matrix at the BS and the reflection coefficients at the RIS. The problem \mathcal{P}_0 can be expressed as

$$\mathcal{P}_1 : \max_{\mathbf{Q}, \Theta} \sum_{i=1}^{N_s} \log_2 \left(1 + \sum_{j=1}^i \frac{1}{P-j+1} \sum_{j=1}^i \frac{1}{L-j+1} \frac{N_b N_u N_r^2}{\sigma^2 P L} d_{b,i} d_{u,i} d_{r,i} \right) \quad (23a)$$

$$\text{s.t.} \quad \text{tr}(\mathbf{Q}) \leq P_T, \quad (23b)$$

$$\mathbf{Q} \succeq 0, \quad (23c)$$

$$\Theta = \text{diag} (e^{j\phi_1}, \dots, e^{j\phi_{N_r}}). \quad (23d)$$

Compared with the original problem \mathcal{P}_0 , the problem \mathcal{P}_1 is much clearer. However, the problem \mathcal{P}_1 is still challenging due to two facts. Firstly, the objective function is not directly related to the optimizing variables \mathbf{Q} and Θ . Thus, we need to bridge the gap for the further optimization procedure. Secondly, the problem \mathcal{P}_1 is highly non-convex due to the unit-modulus constraints. In the following, we will first introduce a theorem to connect the objective function with the optimizing variables. Then, the alternating optimization method is adopted to decouple the problem \mathcal{P}_1 into two sub-problems.

Theorem 3: Let $\mathbf{U} \in \mathbb{C}^{N \times N}$ be unitary matrix, i.e., $\mathbf{U}^H \mathbf{U} = \mathbf{U} \mathbf{U}^H = \mathbf{I}$. If $\mathbf{c} \in \mathbb{R}_+^N$ and $\mathbf{s} \in \mathbb{R}_+^N$ are nonnegative real sequences that are in descending order. Then, we have

$$\det [\mathbf{I} + \text{diag}(\mathbf{c}) \mathbf{U}^H \text{diag}(\mathbf{s}) \mathbf{U}] \leq \det [\mathbf{I} + \mathbf{U}^H \text{diag}(\mathbf{c}) \text{diag}(\mathbf{s}) \mathbf{U}] \quad (24)$$

Proof: See Appendix E. ■

A. Transmit Covariance Matrix Optimization

Define $\beta = \sum_{j=1}^i \frac{1}{P-j+1} \sum_{j=1}^i \frac{1}{L-j+1} \frac{N_b N_u N_r^2}{\sigma^2 P L}$ and $\boldsymbol{\gamma} = \beta \text{diag} (d_{u,1} d_{r,1}, d_{u,2} d_{r,2}, \dots, d_{u,N_s} d_{r,N_s}, 0, \dots, 0) \in \mathbb{R}^{P \times P}$, then we have

$$\begin{aligned} C_{Jen2} &= \sum_{i=1}^{N_s} \log_2 (1 + \beta d_{b,i} d_{u,i} d_{r,i}) \\ &= \log_2 \det [\mathbf{I}_P + \boldsymbol{\gamma} \mathbf{D}_b] \\ &\stackrel{(a)}{\geq} \log_2 \det [\mathbf{I}_P + \boldsymbol{\gamma} \mathbf{U}_b^H \mathbf{D}_b \mathbf{U}_b] \\ &\stackrel{(b)}{=} \log_2 \det [\mathbf{I}_P + \boldsymbol{\gamma} \mathbf{A}_b^H \mathbf{Q} \mathbf{A}_b], \\ &= \log_2 \det \left[\mathbf{I}_P + (\mathbf{A}_b \boldsymbol{\gamma}^{1/2})^H \mathbf{Q} (\mathbf{A}_b \boldsymbol{\gamma}^{1/2}) \right], \end{aligned} \quad (25)$$

where (a) holds due to Theorem 3 and (b) holds due to $\mathbf{A}_b^H \mathbf{Q} \mathbf{A}_b = \mathbf{U}_b^H \mathbf{D}_b \mathbf{U}_b$. Note that we find the lower bound of the approximated ergodic capacity through Theorem 3. Thus, it is reasonable to maximize C_{Jen2} by maximizing its lower bound. Therefore, when fixing the reflection coefficients at the RIS, the problem \mathcal{P}_1 can be expressed as

$$\max_{\mathbf{Q}} \log_2 \det \left[\mathbf{I}_P + (\mathbf{A}_b \gamma^{1/2})^H \mathbf{Q} (\mathbf{A}_b \gamma^{1/2}) \right] \quad (26a)$$

$$\text{s.t.} \quad \text{tr}(\mathbf{Q}) \leq P_T, \quad (26b)$$

$$\mathbf{Q} \succeq 0. \quad (26c)$$

Note that it is a convex optimization problem over \mathbf{Q} and can be optimally solved by the well-know water-filling algorithm. Specifically, define the singular value decomposition (SVD) of $(\mathbf{A}_b \gamma^{1/2})^H$ as

$$(\mathbf{A}_b \gamma^{1/2})^H = \mathbf{U} \mathbf{\Sigma} \mathbf{V}^H = \begin{bmatrix} \mathbf{U}_1 & \mathbf{U}_2 \end{bmatrix} \begin{bmatrix} \mathbf{\Sigma}_1 & \mathbf{0} \\ \mathbf{0} & \mathbf{\Sigma}_2 \end{bmatrix} \begin{bmatrix} \mathbf{V}_1^H \\ \mathbf{V}_2^H \end{bmatrix}, \quad (27)$$

where \mathbf{U} is a $P \times P$ unitary matrix, $\mathbf{\Sigma}$ is a $P \times N_b$ diagonal matrix of singular values, \mathbf{V} is an $N_b \times N_b$ unitary matrix. The truncated SVD of $(\mathbf{A}_b \gamma^{1/2})^H$ is $\mathbf{U}_1 \mathbf{\Sigma}_1 \mathbf{V}_1^H$, where $\mathbf{\Sigma}_1 \in \mathbb{R}^{P \times N_s}$ and $\mathbf{V}_1 \in \mathbb{C}^{N_b \times N_s}$. Thus, the optimal solution to the problem (26) is given by

$$\mathbf{Q}^* = \mathbf{V}_1 \text{diag}(p_1, p_2, \dots, p_{N_s}) \mathbf{V}_1^H, \quad (28)$$

where $p_i = \max(1/p_0 - 1/\Sigma_1^2(i, i), 0)$, $i = 1, 2, \dots, N_s$ denotes the optimal amount of power allocated to the i -th data stream, and p_0 is the water level satisfying $\sum_{i=1}^{N_s} p_i = P_T$.

B. Reflection Coefficients Optimization

Define $\mathbf{\Gamma} = \beta \text{diag}(d_{u,1} d_{b,1}, d_{u,2} d_{b,2}, \dots, d_{u,N_s} d_{b,N_s}, 0, \dots, 0) \in \mathbb{R}^{P \times P}$, similar to the transmit covariance matrix optimization, we have

$$\begin{aligned} C_{Jen2} &= \sum_{i=1}^{N_s} \log_2 (1 + \beta d_{b,i} d_{u,i} d_{r,i}) \\ &= \log_2 \det [\mathbf{I}_P + \mathbf{\Gamma} \mathbf{D}_r] \\ &\stackrel{(a)}{\geq} \log_2 \det [\mathbf{I}_P + \mathbf{\Gamma} \mathbf{U}_r^H \mathbf{D}_r \mathbf{U}_r] \\ &\stackrel{(b)}{=} \log_2 \det [\mathbf{I}_P + \mathbf{\Gamma} \mathbf{X}^H \mathbf{X}], \end{aligned} \quad (29)$$

where (a) holds due to Theorem 3, (b) holds due to $\mathbf{X}^H \mathbf{X} = \mathbf{U}_r^H \mathbf{D}_r \mathbf{U}_r$ and $\mathbf{X} = \mathbf{A}_{rL}^H \boldsymbol{\Theta} \mathbf{A}_{rp}$. Therefore, when fixing the transmit covariance matrix at the BS, the problem \mathcal{P}_1 can be expressed as

$$\max_{\boldsymbol{\Theta}} \quad \log_2 \det [\mathbf{I}_P + \boldsymbol{\Gamma} \mathbf{A}_{rp}^H \boldsymbol{\Theta}^H \mathbf{A}_{rL} \mathbf{A}_{rL}^H \boldsymbol{\Theta} \mathbf{A}_{rp}] \quad (30a)$$

$$\text{s.t.} \quad \boldsymbol{\Theta} = \text{diag} (e^{j\phi_1}, \dots, e^{j\phi_{N_r}}). \quad (30b)$$

The problem (30) is highly non-convex due to the non-convex unit-modulus constraints and the fact that the objective function is not concave with respect to $\boldsymbol{\Theta}$. To the best of the authors' knowledge, there is no general approach to solve the problem (30) optimally. Here, we adopt the RCG algorithm to handle it. The RCG algorithm is widely applied in hybrid beamforming design [22] and recently applied in RIS-aided systems as well [8], [11], [27]. Note that the RCG algorithm is suitable to handle the problems with the unit-modulus constraints, and it usually can carry out a good solution.

Note that the reflection coefficients of the RIS have a diagonal structure. Thus, we introduce a mask matrix \mathbf{I} (\mathbf{I} is an identity matrix). Then, we can rewrite the reflection coefficients of the RIS as $\boldsymbol{\Theta} = \mathbf{I} \odot \tilde{\boldsymbol{\Theta}}$, where $\tilde{\boldsymbol{\Theta}} \in \mathbb{C}^{N_r \times N_r}$ is an auxiliary matrix variable without the diagonal constraint and all of its units satisfy the unit-modulus constraints. Thereby, the feasible set of $\tilde{\boldsymbol{\Theta}}$ forms a Riemannian manifold $\mathcal{M} = \{\tilde{\boldsymbol{\Theta}} \in \mathbb{C}^{N_r \times N_r} : |[\tilde{\boldsymbol{\Theta}}]_{ij}| = 1, \forall i, j\}$ [28]. The main idea of the RCG algorithm is to generalize a conjugate gradient method from the Euclidean space to the manifold space. Here, we start with the definition of the tangent space. The tangent space $T_{\tilde{\boldsymbol{\Theta}}_i} \mathcal{M}$ of the manifold \mathcal{M} at point $\tilde{\boldsymbol{\Theta}}_i$ is given by

$$T_{\tilde{\boldsymbol{\Theta}}_i} \mathcal{M} = \left\{ \mathbf{Z} \in \mathbb{C}^{N_r \times N_r} : \Re \left\{ \mathbf{Z} \odot \tilde{\boldsymbol{\Theta}}_i^* \right\} = \mathbf{0} \right\}. \quad (31)$$

The main procedure of the RCG algorithm consists of three steps in each iteration.

1) *Riemannian Gradient*: The Riemannian gradient is one tangent vector (direction) with the steepest increase of the objective function. Define $\boldsymbol{\Omega} = \mathbf{I}_P + \boldsymbol{\Gamma} \mathbf{A}_{rp}^H \boldsymbol{\Theta}^H \mathbf{A}_{rL} \mathbf{A}_{rL}^H \boldsymbol{\Theta} \mathbf{A}_{rp}$, the Riemannian gradient of the objective function $f(\tilde{\boldsymbol{\Theta}}) = -\log_2 \det(\boldsymbol{\Omega})$ at the point $\tilde{\boldsymbol{\Theta}}_i$, denoted by $\text{grad} f(\tilde{\boldsymbol{\Theta}}_i)$, is given by

$$\text{grad} f(\tilde{\boldsymbol{\Theta}}_i) = \nabla f(\tilde{\boldsymbol{\Theta}}_i) - \Re \left\{ \nabla f(\tilde{\boldsymbol{\Theta}}_i) \odot \tilde{\boldsymbol{\Theta}}_i^* \right\} \odot \tilde{\boldsymbol{\Theta}}_i, \quad (32)$$

where $\nabla f(\tilde{\boldsymbol{\Theta}}_i)$ denotes the Euclidean gradient. In the following, we will compute the Euclidean gradient of the objective function.

Based on the differential rule $d(\det(\mathbf{A})) = \det(\mathbf{A}) \operatorname{tr}(\mathbf{A}^{-1} d(\mathbf{A}))$, we have

$$\begin{aligned}
d\left(f(\tilde{\Theta})\right) &= -d\left(\log_2 \det(\Omega)\right) \\
&= -\frac{1}{\ln 2} \operatorname{tr}(\Omega^{-1} d(\Omega)) \\
&= -\frac{1}{\ln 2} \operatorname{tr}(\Omega^{-1} \Gamma \mathbf{A}_{rp}^H d(\Theta^H) \mathbf{A}_{rL} \mathbf{A}_{rL}^H \Theta \mathbf{A}_{rp}) \\
&\stackrel{(a)}{=} -\frac{1}{\ln 2} \operatorname{tr}(\mathbf{A}_{rL} \mathbf{A}_{rL}^H \Theta \mathbf{A}_{rp} \Omega^{-1} \Gamma \mathbf{A}_{rp}^H d(\Theta^H)) \\
&\stackrel{(b)}{=} -\frac{1}{\ln 2} \operatorname{tr}\left(\left(\mathbf{A}_{rL} \mathbf{A}_{rL}^H \Theta \mathbf{A}_{rp} \Omega^{-1} \Gamma \mathbf{A}_{rp}^H\right) \left(\mathbf{I} \odot d(\tilde{\Theta}^H)\right)\right) \\
&\stackrel{(c)}{=} -\frac{1}{\ln 2} \operatorname{tr}\left(\left(\left(\mathbf{A}_{rL} \mathbf{A}_{rL}^H \Theta \mathbf{A}_{rp} \Omega^{-1} \Gamma \mathbf{A}_{rp}^H\right) \odot \mathbf{I}\right) d(\tilde{\Theta}^H)\right),
\end{aligned} \tag{33}$$

where (a) holds due to $\operatorname{tr}(\mathbf{A}\mathbf{B}) = \operatorname{tr}(\mathbf{B}\mathbf{A})$ for arbitrary matrices \mathbf{A} and \mathbf{B} , (b) holds due to $d(\Theta) = \mathbf{I} \odot d(\tilde{\Theta})$, and (c) holds due to $\operatorname{tr}(\mathbf{A}(\mathbf{B} \odot \mathbf{C})) = \operatorname{tr}((\mathbf{A} \odot \mathbf{B}^T) \mathbf{C})$ for arbitrary matrices \mathbf{A} , \mathbf{B} and \mathbf{C} .

According to the fact that $d\left(f(\tilde{\Theta})\right) = \operatorname{tr}\left(\nabla f(\tilde{\Theta}) d(\tilde{\Theta}^H)\right)$, we obtain the Euclidean gradient of the objective function $f(\tilde{\Theta})$ as

$$\nabla f(\tilde{\Theta}) = -\frac{1}{\ln 2} \left(\mathbf{A}_{rL} \mathbf{A}_{rL}^H \Theta \mathbf{A}_{rp} \Omega^{-1} \Gamma \mathbf{A}_{rp}^H\right) \odot \mathbf{I}. \tag{34}$$

2) *Transport*: With the obtained Riemannian gradient, the optimization tools in the Euclidean space can be extended to the manifold space. However, the search direction $\boldsymbol{\eta}_i$ and $\boldsymbol{\eta}_{i+1}$ usually lie in two different tangent spaces. Therefore, the transport operation $T_{\tilde{\Theta}_i \rightarrow \tilde{\Theta}_{i+1}}(\boldsymbol{\eta}_i)$ is needed to map the tangent vector $\boldsymbol{\eta}_i$ from $T_{\tilde{\Theta}_i} \mathcal{M}$ to $T_{\tilde{\Theta}_{i+1}} \mathcal{M}$, which is given by

$$\begin{aligned}
T_{\tilde{\Theta}_i \rightarrow \tilde{\Theta}_{i+1}}(\boldsymbol{\eta}_i) : T_{\tilde{\Theta}_i} \mathcal{M} &\mapsto T_{\tilde{\Theta}_{i+1}} \mathcal{M} : \\
\boldsymbol{\eta}_i &\mapsto \boldsymbol{\eta}_i - \Re\left\{\boldsymbol{\eta}_i \odot \tilde{\Theta}_{i+1}^*\right\} \odot \tilde{\Theta}_{i+1}.
\end{aligned} \tag{35}$$

Then, we can update the search direction as

$$\boldsymbol{\eta}_{i+1} = -\operatorname{grad} f(\tilde{\Theta}_{i+1}) + \beta_i T_{\tilde{\Theta}_i \rightarrow \tilde{\Theta}_{i+1}}(\boldsymbol{\eta}_i), \tag{36}$$

where β_i is chosen as the Polak-Ribiere parameter [28].

3) *Retraction*: After determining the search direction $\boldsymbol{\eta}_i$, we need to determine the step size α_i . However, the obtained point $\alpha_i \boldsymbol{\eta}_i$ may leave the manifold. Thereby, an operation called *retraction*

Algorithm 1 RCG Algorithm for Reflection Coefficients Optimization

- 1: **Input:** $\{\Gamma, \mathbf{A}_{rp}, \mathbf{A}_{rL}\}$, desired accuracy ϵ
 - 2: Initialize: $\tilde{\Theta}_0, \boldsymbol{\eta}_0 = -\text{grad } f(\tilde{\Theta}_0)$, and set $i = 0$;
 - 3: **repeat**
 - 4: Choose the Armijo backtracking line search step size α_i ;
 - 5: Find the next point $\tilde{\Theta}_{i+1}$ using retraction in (37): $\tilde{\Theta}_{i+1} = \mathcal{R}_{\tilde{\Theta}_i}(\alpha_i \boldsymbol{\eta}_i)$;
 - 6: Calculate the Euclidean gradient $\nabla f(\tilde{\Theta}_{i+1})$ according to (34);
 - 7: Calculate the Riemannian gradient $\text{grad } f(\tilde{\Theta}_{i+1})$ according to (32);
 - 8: Calculate the transport $\mathcal{T}_{\tilde{\Theta}_i \rightarrow \tilde{\Theta}_{i+1}}(\boldsymbol{\eta}_i)$ according to (35);
 - 9: Calculate the conjugate direction $\boldsymbol{\eta}_{i+1}$ according to (36);
 - 10: $i \leftarrow i + 1$;
 - 11: **until** $\|\text{grad } f(\tilde{\Theta}_i)\|_2 \leq \epsilon$.
 - 12: **Output:** $\tilde{\Theta}^* = \tilde{\Theta}_i, \Theta^* = \mathbf{I} \odot \tilde{\Theta}^*$.
-

is needed to map it from the tangent space to the manifold itself, which is given by

$$\mathcal{R}_{\tilde{\Theta}_i}(\alpha_i \boldsymbol{\eta}_i) : T_{\tilde{\Theta}_i} \mathcal{M} \mapsto \mathcal{M} : \quad (37)$$

$$\alpha_i \boldsymbol{\eta}_i \mapsto \frac{\left(\tilde{\Theta}_i + \alpha_i \boldsymbol{\eta}_i \right)_j}{\left| \left(\tilde{\Theta}_i + \alpha_i \boldsymbol{\eta}_i \right)_j \right|},$$

where $\left(\tilde{\Theta}_i + \alpha_i \boldsymbol{\eta}_i \right)_j$ denotes the j -th entry of $\tilde{\Theta}_i + \alpha_i \boldsymbol{\eta}_i$.

The key steps used in each iteration of the manifold optimization are introduced above, and the consequent algorithm for reflection coefficients optimization is summarized in **Algorithm 1**.

Algorithm 1 is guaranteed to converge to a stationary point [28].

C. Overall Algorithm

In the above two subsections, the transmit covariance matrix and the reflection coefficients are optimized in each sub-problem. Here, we propose the overall alternating optimization algorithm for problem \mathcal{P}_1 in **Algorithm 2**. Firstly, the transmit covariance matrix $\mathbf{Q}^{(0)}$ is initialized as an identity matrix, and the reflection coefficients $\Theta^{(1)}$ is obtained based on **Algorithm 1**. Then, the transmit covariance matrix $\mathbf{Q}^{(1)}$ is updated according to (28) with fixed $\Theta^{(1)}$. In each iteration,

Algorithm 2 Alternating Optimization Algorithm for Problem \mathcal{P}_1

- 1: Initialize: $\mathbf{Q}^{(0)} = \frac{P_T}{N_b} \mathbf{I}_{N_b}$, $\Theta^{(0)}$ is randomly generated where the phases $\{\theta_l\}_{\forall l}$ are uniformly and independently distributed in $[0, 2\pi)$, error tolerance ϵ , and set $i = 0$;
 - 2: **repeat**
 - 3: Calculate $\mathbf{Q}^{(i+1)}$ according to (28) with fixed $\Theta^{(i)}$;
 - 4: Calculate $\Theta^{(i+1)}$ based on **Algorithm 1** with fixed $\mathbf{Q}^{(i+1)}$;
 - 5: $i \leftarrow i + 1$;
 - 6: **until** The increase of the objective value of the problem \mathcal{P}_1 is below the threshold ϵ .
-

the lower bound of the objective value of problem \mathcal{P}_1 is maximized. Thus, the objective value of problem \mathcal{P}_1 is non-decreasing over iterations. Therefore, by iteratively calculating $\mathbf{Q}^{(i+1)}$ and $\Theta^{(i+1)}$, our proposed algorithm is guaranteed to converge.

Now, let us consider the complexity of the proposed **Algorithm 2**. Firstly, the complexity of the water-filling algorithm is $\mathcal{O}(PN_b \min(P, N_b)) = \mathcal{O}(N_b)$. Secondly, the complexity of the RCG algorithm is dominated by calculating the Euclidean gradient (34). Define $\Xi_1 = \mathbf{A}_{rL}^H \Theta \mathbf{A}_{rp} \Omega^{-1} \Gamma$ and $\Xi_2 = \mathbf{A}_{rL} \Xi_1 \mathbf{A}_{rp}^H$. Note that only the diagonal elements of Ξ_2 need to be calculated, and the i -th diagonal element of Ξ_2 can be calculated by multiplying the i -th row of \mathbf{A}_{rL} , Ξ_1 and the i -th column of \mathbf{A}_{rp}^H . Thus, the complexity of **Algorithm 1** is $\mathcal{O}(N_r I_1)$, where I_1 denotes the number of iterations of the RCG algorithm. Therefore, the overall complexity is $\mathcal{O}((N_b + N_r I_1) I_2)$, where I_2 denotes the number of iterations of **Algorithm 2**.

V. SIMULATION RESULTS

In this section, we first investigate the tightness of the derived ergodic capacity approximation through Monte-Carlo simulations, then evaluate the performance of the proposed algorithms. We adopt the widely used SV channel model illustrated in Section II-A. The angles $\phi_{b,i}$ and $\psi_{u,i}$ are randomly generated and uniformly distributed in $[-\pi, \pi)$, $\phi_{r,i}^1$ and $\varphi_{r,i}^1$ in $[-\pi/2, \pi/2]$, and $\phi_{r,i}^2$ and $\varphi_{r,i}^2$ in $[0, \pi]$. Other system parameters are set as follows unless specified otherwise later: $N_b = 16$, $N_r = 8 \times 8$, $N_u = 16$. In the first part, we set $\mathbf{Q} = \frac{P_T}{N_b} \mathbf{I}_{N_b}$ and Θ is randomly generated where the phases $\{\theta_l\}_{\forall l}$ are uniformly and independently distributed in $[0, 2\pi)$. All simulation curves are averaged over 1000 independent channel realizations.

A. Tightness of the Derived Ergodic Capacity Approximation

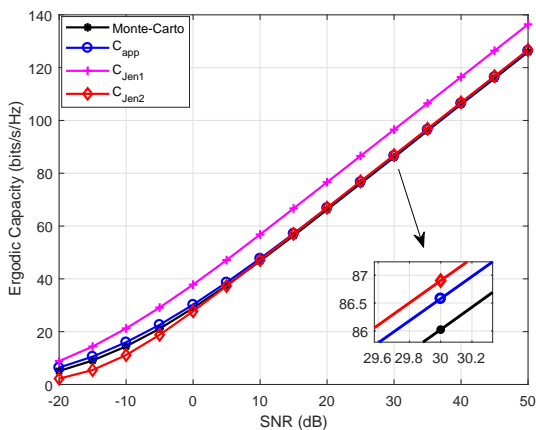


Fig. 2: Ergodic capacity against the transmit SNR with $P = 6$ and $L = 8$.

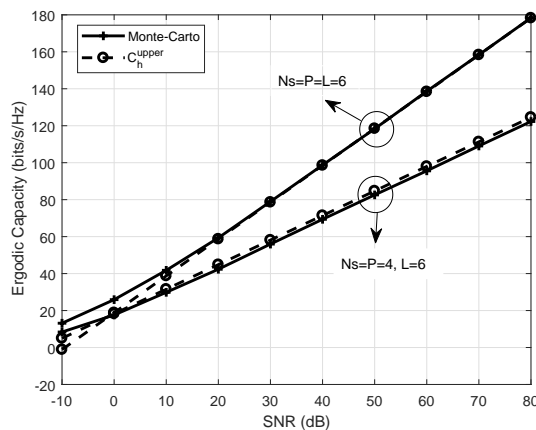


Fig. 3: Capacity upper bound in the high-SNR regime against the transmit SNR.

Fig. 2 illustrates the ergodic capacity against the transmit SNR. Firstly, it is found that C_{app} fits the Monte-Carlo results well. However, there are complex integral items involved in C_{app} , which is not convenient for analysis and optimization. Secondly, C_{Jen1} is much larger than the Monte-Carlo results because it is amplified by the Jensen's inequality. Finally, C_{Jen2} approximates the Monte-Carlo well though it is slightly smaller than the Monte-Carlo results in low-SNR regime. In addition, C_{Jen2} has a very concise expression form. Therefore, it is reasonable to adopt C_{Jen2} to approximate the ergodic capacity in the optimization.

Fig. 3 provides the ergodic capacity upper bound in the high-SNR regime against the transmit SNR. It is found that when SNR is low, C_h^{upper} is much smaller than the Monte-Carlo results. When SNR becomes large, the Monte-Carlo results are bounded by C_h^{upper} , which verifies **Proposition 2**. Specifically, C_h^{upper} is the same as the Monte-Carlo results when $N_s = P = L$ and the SNR is larger than 30 dB.

Fig. 4 shows the ergodic capacity upper bound C_h^{upper} against the number of antennas or reflection units. The leftmost point in this figure is plotted when $N_b = N_r = N_u = 10$, and the other points correspond to the case where one of the three parameters above increases to (20, 40, 80, 160, 320, 640) while the other two remain at 10. Particularly, the RIS is equipped with $N_r^1 \times N_r^2$ unit cells where $N_r^1 = 10$ and N_r^2 can vary. It is found that the ergodic capacity

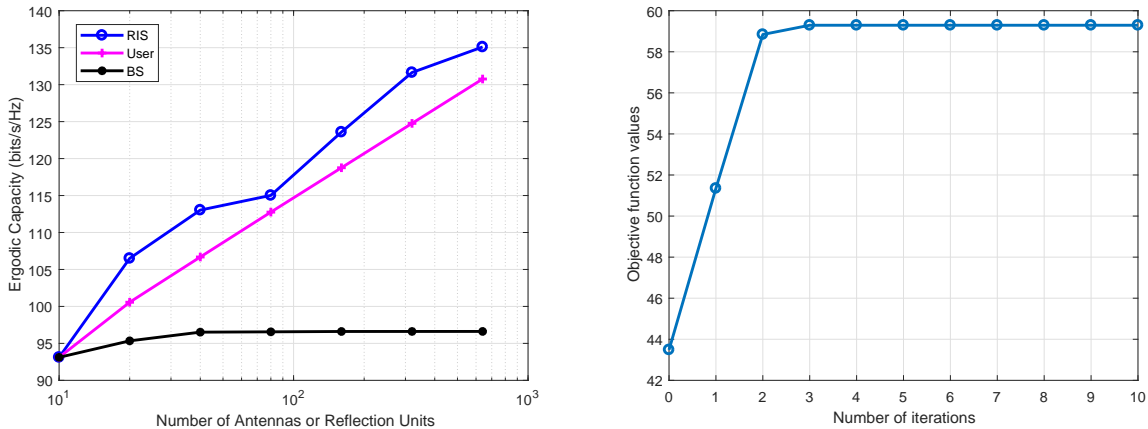


Fig. 4: Ergodic capacity upper bound against the number of antennas or reflection units with SNR = 10 dB, $P = 6$, and $L = 8$.
 SNR = 50 dB, $P = 6$ and $L = 6$.

increases logarithmically with the number of antennas at the user and the number of reflection units at the RIS. Note that the fluctuation of the curve of the RIS is due to the randomly generated reflection coefficients of the RIS. Furthermore, the ergodic capacity is nearly unchanged when the number of antennas at the BS exceeds 40. It is because the eigenvalues of $\mathbf{A}_b^H \mathbf{A}_b$ are nearly unchanged when the number of antennas at the BS is very large. Thus, the ergodic capacity can not be improved by increasing the number of antennas at the BS.

B. Performance of the Proposed Algorithms

Fig. 5 illustrates the convergence performance of the proposed **Algorithm 2**. It can be found that the proposed algorithm converges within 10 iterations, which verifies the convergence of the proposed algorithm.

In Fig. 6, we compare the proposed algorithm with two state-of-the-art benchmarks that assume the knowledge of perfect instantaneous CSI.

- Alternating optimization based algorithm (AO) [10]: The transmit covariance matrix \mathbf{Q} and each unit of the reflection coefficients of the RIS $\{\theta_i\}_{\forall i}$ are alternately optimized until convergence. Note that the closed-form solution at each step is obtained.
- Truncated-SVD-based beamforming (T-SVD-BF) [11]: By exploiting the sparse structure of

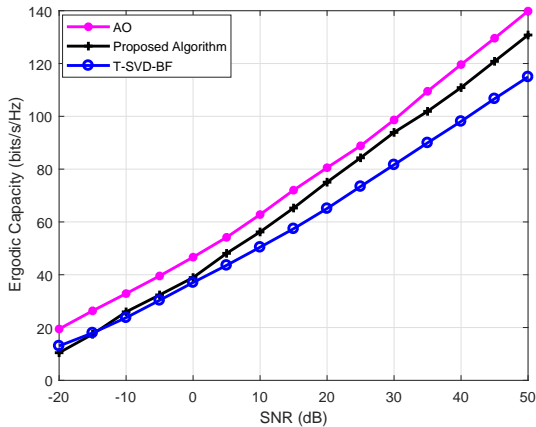


Fig. 6: Performance comparison with benchmarks when $P = 6$ and $L = 8$.

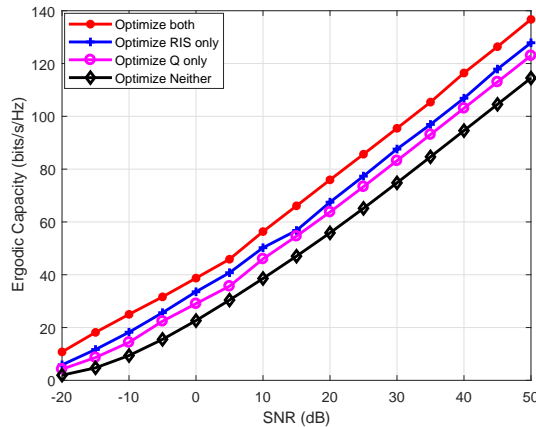


Fig. 7: Influence comparison between transmit covariance matrix and reflection coefficients with $N_b = 16$, $N_r = 64$, $N_u = 16$, $P = 6$ and $L = 8$.

the mmWave communication, work [11] first proposes a manifold-based method to optimize the reflection coefficients of the RIS, then adopts the water-filling algorithm to handle the active beamforming at the BS. Note that no alternating process is needed and each step only needs to be executed once.

It is found that our proposed algorithm outperforms T-SVD-BF and performs a little worse than the AO-based algorithm. When SNR is low, our proposed algorithm performs much worse than the AO-based algorithm because C_{Jen2} is a little smaller than the Monte-Carlo results in low-SNR regime as shown in Fig. 2. The AO-based algorithm performs best because it has closed-form solution in each step and converges to a stationary point. However, when the number of reflection units of the RIS is large, its computational complexity is very high, which is not suitable in practice. The T-SVD-BF method exploits the sparse structure of the mmWave communication and runs very fast. However, its performance is the worst. Note that both the AO-based algorithm and the T-SVD-BF method need perfect instantaneous CSI, which is difficult to obtain. Nevertheless, our proposed algorithm only needs the statistical CSI and its performance is attractive.

In addition, we compare the influence on ergodic capacity of transmit covariance matrix and

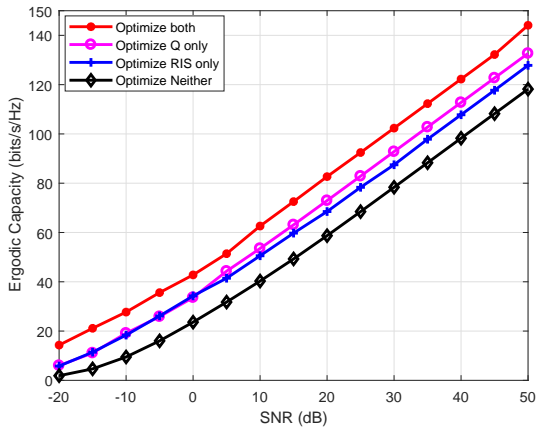


Fig. 8: Influence comparison between transmit covariance matrix and reflection coefficients covariance matrix and reflection coefficients with $N_b = 32$, $N_r = 64$, $N_u = 16$, $P = 6$ and $L = 8$.

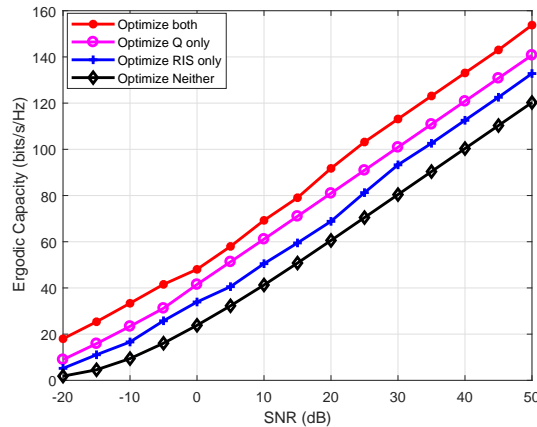


Fig. 9: Influence comparison between transmit covariance matrix and reflection coefficients covariance matrix and reflection coefficients with $N_b = 64$, $N_r = 64$, $N_u = 16$, $P = 6$ and $L = 8$.

reflection coefficients in Fig. 7 - 9. The only difference among them is the number of antennas at the BS, which changes from 16, 32 to 64. The curve “Optimize RIS only” indicates that $\mathbf{Q} = \frac{P_T}{N_b} \mathbf{I}_{N_b}$. The curve “Optimize Q only” indicates that Θ is randomly generated by setting the phases $\{\theta_l\}_{\forall l}$ as uniformly and independently distributed in $[0, 2\pi)$. Firstly, it is found that the ergodic capacity after optimization is about 20 bits/s/Hz higher than that before optimization on average, which verifies the effectiveness of the optimization. Secondly, we observe that when $N_b = 16$, the curve “Optimize RIS only” outperforms the curve “Optimize Q only”. However, when $N_b = 32$ and $N_b = 64$, the curve “Optimize RIS only” performs worse than the curve “Optimize Q only” and the gap enlarges. Thus, with the same number of antennas at the BS and reflection coefficients at the RIS, optimizing the transmit covariance matrix at the BS is superior to optimizing the reflection coefficients at the RIS. When the number of reflection coefficients is much larger than the number of antennas, optimizing the reflection coefficients outperforms optimizing the transmit covariance matrix. Thanks to the low cost of the RIS elements, the RIS is usually composed of a large number of reflection units. In this case, the systems still perform well when the CSI is not available at the BS and the reflection coefficients at the RIS is optimized.

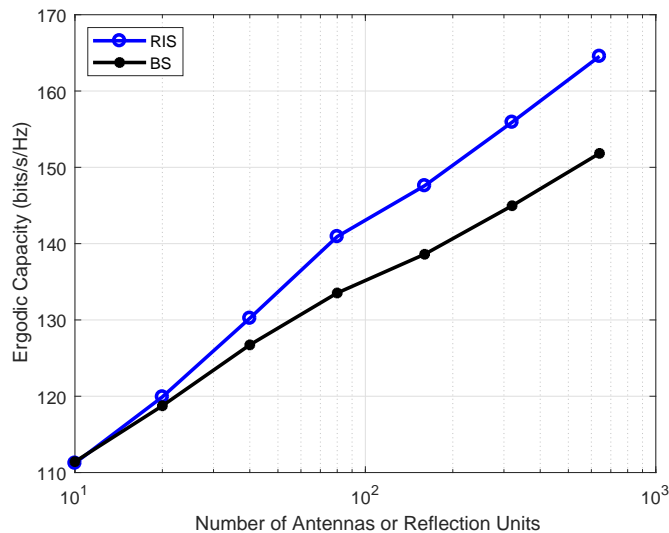


Fig. 10: Ergodic capacity against the number of antennas or reflection units with SNR = 50 dB, $P = L = 6$.

Finally, Fig. 10 depicts the ergodic capacity against the number of antennas or reflection units. The system parameter settings are the same as those of Fig. 4, while the proposed algorithm is adopted in Fig. 10. Compared with Fig. 4, it is interesting to find that the ergodic capacity increases logarithmically with the number of antennas at the BS when the transmit covariance matrix is optimized. Thus, the optimization of the transmit covariance matrix is very important in the RIS-aided mmWave MIMO systems.

VI. CONCLUSION

In this paper, we considered the ergodic capacity of an RIS-aided mmWave MIMO communication system under the SV channel models. The ergodic capacity approximation was derived by means of majorization theory. We also derived the upper bound of the ergodic capacity in high-SNR regime. Based on the derived approximation, we maximized the ergodic capacity by jointly designing the transmit covariance and reflection coefficients at BS and RIS, respectively. Numerical results proved the tightness of the derived ergodic capacity approximation. It was found that the ergodic capacity after optimization could be improved by about 20 bits/s/Hz, which verified the effectiveness of the optimization. In addition, when the BS allocated equal power over transmit signals, the ergodic capacity remained unchanged after the number of antennas at

the BS reached a certain amount. Moreover, it was revealed that if we were allowed to optimize either the transmit covariance matrix or the reflection coefficients, optimizing the reflection coefficients was more effective than optimizing the transmit covariance matrix only in the case of a large number of reflection units. The analysis and results in this article provided insights on the deployment and capacity evaluation of RIS-assisted mmWave wireless systems. Future work may consider the situation with multiple users and RISs.

APPENDIX

A. Proof of Theorem 1

$$\begin{aligned}
C &= \mathbb{E}_{\mathbf{H}} \left[\log_2 \det \left(\mathbf{I}_{N_u} + \frac{1}{\sigma^2} \mathbf{H} \mathbf{Q} \mathbf{H}^H \right) \right] \\
&= \mathbb{E}_{\mathbf{H}} \left[\log_2 \det \left(\mathbf{I}_{N_u} + \frac{1}{\sigma^2} \mathbf{T} \Theta \mathbf{G} \mathbf{Q} \mathbf{G}^H \Theta^H \mathbf{T}^H \right) \right] \\
&= \mathbb{E}_{\mathbf{H}} \left[\log_2 \det \left(\mathbf{I}_{N_u} + \frac{1}{\sigma^2} \mathbf{A}_u \mathbf{T}_L \mathbf{A}_{rL}^H \Theta \mathbf{A}_{rp} \mathbf{G}_p \mathbf{A}_b^H \mathbf{Q} \mathbf{A}_b \mathbf{G}_p^H \mathbf{A}_{rp}^H \Theta^H \mathbf{A}_{rL} \mathbf{T}_L^H \mathbf{A}_u^H \right) \right] \\
&= \mathbb{E}_{\mathbf{H}} \left[\log_2 \det \left[\prod_{i=1}^{N_u} \left(1 + \frac{1}{\sigma^2} \lambda_i \left(\mathbf{A}_u \mathbf{T}_L \mathbf{A}_{rL}^H \Theta \mathbf{A}_{rp} \mathbf{G}_p \mathbf{A}_b^H \mathbf{Q} \mathbf{A}_b \mathbf{G}_p^H \mathbf{A}_{rp}^H \Theta^H \mathbf{A}_{rL} \mathbf{T}_L^H \mathbf{A}_u^H \right) \right) \right] \right], \tag{38}
\end{aligned}$$

where $\lambda_i(\cdot)$ denotes the i -th largest eigenvalue of the input matrix.

According to the definition [[29], 1.A.7], $\forall \mathbf{x}, \mathbf{y} \in \mathbb{R}_+^n$, \mathbf{x} is said to be log-majorized by \mathbf{y} , denoted by $\mathbf{x} \prec_{\log} \mathbf{y}$, if

$$\begin{aligned}
\prod_{i=1}^k x_{[i]} &\leq \prod_{i=1}^k y_{[i]}, \quad k = 1, \dots, n-1, \\
\prod_{i=1}^n x_{[i]} &= \prod_{i=1}^n y_{[i]}.
\end{aligned} \tag{39}$$

According to [[29], Theorem 9.H.1.a] If \mathbf{U} and \mathbf{V} are $n \times n$ positive semidefinite Hermitian matrices, then

$$\begin{aligned}
\prod_{i=1}^k \lambda_i(\mathbf{UV}) &\leq \prod_{i=1}^k \lambda_i(\mathbf{U}) \lambda_i(\mathbf{V}), \quad k = 1, \dots, n-1, \\
\prod_{i=1}^n \lambda_i(\mathbf{UV}) &= \prod_{i=1}^n \lambda_i(\mathbf{U}) \lambda_i(\mathbf{V}).
\end{aligned} \tag{40}$$

Thus, $\lambda(\mathbf{UV}) \prec_{\log} \lambda(\mathbf{U}) \odot \lambda(\mathbf{V})$, where \odot denotes hadamard product, and $\lambda(\mathbf{Y}) = [\lambda_1(\mathbf{Y}), \lambda_2(\mathbf{Y}), \dots, \lambda_n(\mathbf{Y})]^T$, $\mathbf{Y} \in \{\mathbf{UV}, \mathbf{U}, \mathbf{V}\}$. Therefore, we can obtain

$$\begin{aligned} & \lambda(\mathbf{A}_u \mathbf{T}_L \mathbf{A}_{rL}^H \Theta \mathbf{A}_{rp} \mathbf{G}_p \mathbf{A}_b^H \mathbf{Q} \mathbf{A}_b \mathbf{G}_p^H \mathbf{A}_{rp}^H \Theta^H \mathbf{A}_{rL} \mathbf{T}_L^H \mathbf{A}_u^H) \\ & \stackrel{(a)}{\prec}_{\log} \lambda(\mathbf{A}_u \mathbf{A}_u^H) \odot \lambda(\mathbf{T}_L \mathbf{A}_{rL}^H \Theta \mathbf{A}_{rp} \mathbf{G}_p \mathbf{A}_b^H \mathbf{Q} \mathbf{A}_b \mathbf{G}_p^H \mathbf{A}_{rp}^H \Theta^H \mathbf{A}_{rL} \mathbf{T}_L^H) \\ & \stackrel{(b)}{\prec}_{\log} \lambda(\mathbf{A}_u^H \mathbf{A}_u) \odot \lambda(\mathbf{A}_b^H \mathbf{Q} \mathbf{A}_b) \odot \lambda(\mathbf{X}^H \mathbf{X}) \odot \lambda(\mathbf{G}_p^H \mathbf{G}_p) \odot \lambda(\mathbf{T}_L^H \mathbf{T}_L), \end{aligned} \quad (41)$$

where (a) follows $\lambda(\mathbf{AB}) = \lambda(\mathbf{BA})$, (b) follows applying Theorem in (40) repeatedly, and $\mathbf{X} = \mathbf{A}_{rL}^H \Theta \mathbf{A}_{rp}$.

According to definition [[29], 1.A.2], $\forall \mathbf{x}, \mathbf{y} \in \mathbb{R}^n$, \mathbf{x} is said to be weakly majorized by \mathbf{y} , denoted by $\mathbf{x} \prec_w \mathbf{y}$, if

$$\sum_{i=1}^k x[i] \leq \sum_{i=1}^k y[i], \quad k = 1, \dots, n-1. \quad (42)$$

According to [[30], Theorem 2.7], Let the components of $\mathbf{x}, \mathbf{y} \in \mathbb{R}^n$ be nonnegative. Then

$$\mathbf{x} \prec_{\log} \mathbf{y} \quad \text{implies} \quad \mathbf{x} \prec_w \mathbf{y}. \quad (43)$$

Thus, (41) can be further simplified as

$$\begin{aligned} & \lambda(\mathbf{A}_u \mathbf{T}_L \mathbf{A}_{rL}^H \Theta \mathbf{A}_{rp} \mathbf{G}_p \mathbf{A}_b^H \mathbf{Q} \mathbf{A}_b \mathbf{G}_p^H \mathbf{A}_{rp}^H \Theta^H \mathbf{A}_{rL} \mathbf{T}_L^H \mathbf{A}_u^H) \\ & \prec_w \lambda(\mathbf{A}_u^H \mathbf{A}_u) \odot \lambda(\mathbf{A}_b^H \mathbf{Q} \mathbf{A}_b) \odot \lambda(\mathbf{X}^H \mathbf{X}) \odot \lambda(\mathbf{G}_p^H \mathbf{G}_p) \odot \lambda(\mathbf{T}_L^H \mathbf{T}_L). \end{aligned} \quad (44)$$

According to [[29], 1.A.1], $\forall \mathbf{x}, \mathbf{y} \in \mathbb{R}^n$, \mathbf{x} is said to be majorized by \mathbf{y} , denoted by $\mathbf{x} \prec \mathbf{y}$, if

$$\begin{aligned} & \sum_{i=1}^k x[i] \leq \sum_{i=1}^k y[i], \quad k = 1, \dots, n-1, \\ & \sum_{i=1}^n x[i] = \sum_{i=1}^n y[i]. \end{aligned} \quad (45)$$

According to [[29], 3.C.1], if $\mathbf{I} \subset \mathbb{R}$ is an interval and $g : \mathbf{I} \rightarrow \mathbb{R}$ is convex, then

$$\phi(\mathbf{x}) = \sum_{i=1}^n g(x_i) \quad (46)$$

is Schur-convex on \mathbf{I}^n . Consequently, $\mathbf{x} \prec \mathbf{y}$ on \mathbf{I}^n implies $\phi(\mathbf{x}) \leq \phi(\mathbf{y})$. Similarly, if g is concave, the $\phi(\mathbf{x})$ is Schur-concave.

According to [[29], 5.A.9], $\forall \mathbf{x}, \mathbf{y} \in \mathbb{R}^n$, if $\mathbf{x} \prec_w \mathbf{y}$, then there exists a vector \mathbf{u} such that $\mathbf{x} \leq \mathbf{u}$ and $\mathbf{u} \prec \mathbf{y}$.

Thus, there exists a vector \mathbf{u} such that

$$\lambda(\mathbf{A}_u \mathbf{T}_L \mathbf{A}_{rL}^H \Theta \mathbf{A}_{rp} \mathbf{G}_p \mathbf{A}_b^H \mathbf{Q} \mathbf{A}_b \mathbf{G}_p^H \mathbf{A}_{rp}^H \Theta^H \mathbf{A}_{rL} \mathbf{T}_L^H \mathbf{A}_u^H) \leq \mathbf{u}, \quad (47a)$$

$$\mathbf{u} \prec \lambda(\mathbf{A}_u^H \mathbf{A}_u) \odot \lambda(\mathbf{A}_b^H \mathbf{Q} \mathbf{A}_b) \odot \lambda(\mathbf{X}^H \mathbf{X}) \odot \lambda(\mathbf{G}_p^H \mathbf{G}_p) \odot \lambda(\mathbf{T}_L^H \mathbf{T}_L) \quad (47b)$$

Define $g(\lambda) = \log_2(1 + \frac{1}{\sigma^2} \lambda)$ and $\phi(\boldsymbol{\lambda}) = \sum_{i=1}^{N_s} g(\lambda_i)$, then $g(\lambda)$ is an increasing concave function. According to (46), $\phi(\boldsymbol{\lambda})$ is an increasing Schur-concave function. Then, we have

$$\phi(\lambda(\mathbf{A}_u \mathbf{T}_L \mathbf{A}_{rL}^H \Theta \mathbf{A}_{rp} \mathbf{G}_p \mathbf{A}_b^H \mathbf{Q} \mathbf{A}_b \mathbf{G}_p^H \mathbf{A}_{rp}^H \Theta^H \mathbf{A}_{rL} \mathbf{T}_L^H \mathbf{A}_u^H)) \leq \phi(\mathbf{u}), \quad (48)$$

and

$$\phi(\lambda(\mathbf{A}_u^H \mathbf{A}_u) \odot \lambda(\mathbf{A}_b^H \mathbf{Q} \mathbf{A}_b) \odot \lambda(\mathbf{X}^H \mathbf{X}) \odot \lambda(\mathbf{G}_p^H \mathbf{G}_p) \odot \lambda(\mathbf{T}_L^H \mathbf{T}_L)) \leq \phi(\mathbf{u}). \quad (49)$$

Therefore, combining (48) and (49), we have

$$\begin{aligned} & \phi(\lambda(\mathbf{A}_u \mathbf{T}_L \mathbf{A}_{rL}^H \Theta \mathbf{A}_{rp} \mathbf{G}_p \mathbf{A}_b^H \mathbf{Q} \mathbf{A}_b \mathbf{G}_p^H \mathbf{A}_{rp}^H \Theta^H \mathbf{A}_{rL} \mathbf{T}_L^H \mathbf{A}_u^H)) \\ & \approx \phi(\lambda(\mathbf{A}_u^H \mathbf{A}_u) \odot \lambda(\mathbf{A}_b^H \mathbf{Q} \mathbf{A}_b) \odot \lambda(\mathbf{X}^H \mathbf{X}) \odot \lambda(\mathbf{G}_p^H \mathbf{G}_p) \odot \lambda(\mathbf{T}_L^H \mathbf{T}_L)). \end{aligned} \quad (50)$$

Assume the eigenvalue decompositions (EVD) of $\mathbf{A}_u^H \mathbf{A}_u$, $\mathbf{A}_b^H \mathbf{Q} \mathbf{A}_b$ and $\mathbf{X}^H \mathbf{X}$ can be expressed as following,

$$\begin{aligned} \mathbf{A}_u^H \mathbf{A}_u &= \mathbf{U}_u^H \mathbf{D}_u \mathbf{U}_u, \\ \mathbf{A}_b^H \mathbf{Q} \mathbf{A}_b &= \mathbf{U}_b^H \mathbf{D}_b \mathbf{U}_b, \\ \mathbf{X}^H \mathbf{X} &= \mathbf{U}_r^H \mathbf{D}_r \mathbf{U}_r, \end{aligned} \quad (51)$$

where \mathbf{U}_u , \mathbf{U}_b , and \mathbf{U}_r are the eigenvectors of $\mathbf{A}_u^H \mathbf{A}_u$, $\mathbf{A}_b^H \mathbf{Q} \mathbf{A}_b$, and $\mathbf{X}^H \mathbf{X}$, respectively; $\mathbf{D}_u = \text{diag}(d_{u,1}, d_{u,2}, \dots, d_{u,L})$, $\mathbf{D}_b = \text{diag}(d_{b,1}, d_{b,2}, \dots, d_{b,P})$, $\mathbf{D}_r = \text{diag}(d_{r,1}, d_{r,2}, \dots, d_{r,P})$, and $d_{u,i}, d_{b,i}, d_{r,i} \geq 0$ are the eigenvalue of $\mathbf{A}_u^H \mathbf{A}_u$, $\mathbf{A}_b^H \mathbf{Q} \mathbf{A}_b$, and $\mathbf{X}^H \mathbf{X}$ in descending order, respectively.

Then, the ergodic capacity C (38) can be approximated by

$$\begin{aligned} C_{app} &= \mathbb{E}_\lambda \left[\log_2 \det \left(\mathbf{I}_{N_s} + \frac{1}{\sigma^2} \lambda(\mathbf{A}_u^H \mathbf{A}_u) \odot \lambda(\mathbf{A}_b^H \mathbf{Q} \mathbf{A}_b) \odot \lambda(\mathbf{X}^H \mathbf{X}) \odot \lambda(\mathbf{G}_p^H \mathbf{G}_p) \odot \lambda(\mathbf{T}_L^H \mathbf{T}_L) \right) \right] \\ &\stackrel{(a)}{=} \mathbb{E}_{g,t} \left[\sum_{i=1}^{N_s} \log_2 \left(1 + \frac{N_b N_u N_r^2}{\sigma^2 P L} d_{b,i} d_{u,i} d_{r,i} |g_i|^2 |t_i|^2 \right) \right], \end{aligned} \quad (52)$$

where $N_s = \min(\text{rank}(\mathbf{A}_b^H \mathbf{Q} \mathbf{A}_b), \text{rank}(\mathbf{A}_u^H \mathbf{A}_u), \text{rank}(\mathbf{X}^H \mathbf{X}))$ denotes the data streams, (a) follows $\lambda(\mathbf{G}_p^H \mathbf{G}_p) = \frac{N_b N_r}{P} [|g_1|^2, |g_2|^2, \dots, |g_P|^2]^T$ and $\lambda(\mathbf{T}_L^H \mathbf{T}_L) = \frac{N_u N_r}{L} [|t_1|^2, |t_2|^2, \dots, |t_L|^2]^T$.

B. Proof of Proposition 1

Since \mathbf{A}_b , \mathbf{A}_u , \mathbf{A}_{rp} and \mathbf{A}_{rL} are composed of the columns of unitary matrices, the AOA at the RIS is symmetric to the AOD at the RIS, $\mathbf{Q} = \frac{P_T}{N_b} \mathbf{I}_{N_b}$, and $\mathbf{\Theta} = \mathbf{I}_{N_r}$, then $\mathbf{A}_b^H \mathbf{Q} \mathbf{A}_b = \frac{P_T}{N_b} \mathbf{I}_P$, $\mathbf{A}_u^H \mathbf{A}_u = \mathbf{I}_L$ and $\mathbf{X} = \mathbf{A}_{rL}^H \mathbf{\Theta} \mathbf{A}_{rp} = \mathbf{I}_{L \times P}$. Thus, the ergodic capacity (9) can be expressed as

$$\begin{aligned}
C_{exact} &= \mathbb{E}_{\mathbf{H}} \left[\log_2 \det \left(\mathbf{I}_{N_u} + \frac{1}{\sigma^2} \mathbf{H} \mathbf{Q} \mathbf{H}^H \right) \right] \\
&= \mathbb{E}_{\mathbf{G}_p, \mathbf{T}_L} \left[\log_2 \det \left(\mathbf{I}_{N_u} + \frac{1}{\sigma^2} \mathbf{A}_u \mathbf{T}_L \mathbf{A}_{rL}^H \mathbf{\Theta} \mathbf{A}_{rp} \mathbf{G}_p \mathbf{A}_b^H \mathbf{Q} \mathbf{A}_b \mathbf{G}_p^H \mathbf{A}_{rp}^H \mathbf{\Theta}^H \mathbf{A}_{rL} \mathbf{T}_L^H \mathbf{A}_u^H \right) \right] \\
&= \mathbb{E}_{\mathbf{G}_p, \mathbf{T}_L} \left[\log_2 \det \left(\mathbf{I}_{N_u} + \frac{P_T}{\sigma^2 N_b} \mathbf{I}_{L \times P} \mathbf{G}_p \mathbf{G}_p^H \mathbf{I}_{P \times L} \mathbf{T}_L^H \mathbf{T}_L \right) \right] \\
&\stackrel{(a)}{=} \mathbb{E}_{g,t} \left[\sum_{i=1}^{N_s} \log_2 \left(1 + \frac{P_T N_u N_r^2}{\sigma^2 P L} |g_i|^2 |t_i|^2 \right) \right], \tag{53}
\end{aligned}$$

where (a) holds due to $\mathbf{G}_p = \sqrt{\frac{N_r N_b}{P}} \text{diag}(g_1, g_2, \dots, g_P)$ and $\mathbf{T}_L = \sqrt{\frac{N_r N_u}{L}} \text{diag}(t_1, t_2, \dots, t_L)$. At the same time, we have $d_{b,i} = \frac{P_T}{N_b}$, $d_{u,i} = 1$, $d_{r,i} = 1$, $i = 1, 2, \dots, N_s$ due to the fact that $\mathbf{A}_b^H \mathbf{Q} \mathbf{A}_b = \frac{P_T}{N_b} \mathbf{I}_P$, $\mathbf{A}_u^H \mathbf{A}_u = \mathbf{I}_L$ and $\mathbf{X} = \mathbf{A}_{rL}^H \mathbf{\Theta} \mathbf{A}_{rp} = \mathbf{I}_{L \times P}$. Therefore, the ergodic capacity approximation (11) can be rewritten as

$$C_{app} = \mathbb{E}_{g,t} \left[\sum_{i=1}^{N_s} \log_2 \left(1 + \frac{P_T N_u N_r^2}{\sigma^2 P L} |g_i|^2 |t_i|^2 \right) \right]. \tag{54}$$

Consequently, the derived ergodic capacity approximation is identical to the exact ergodic capacity.

C. Proof of Proposition 2

The ergodic capacity in (38) of the RIS-aided mmWave MIMO communication systems can be expressed as

$$\begin{aligned}
C &= \mathbb{E}_{\mathbf{H}} \left[\log_2 \det \left(\mathbf{I}_L + \frac{1}{\sigma^2} \mathbf{T}_L \mathbf{A}_{rL}^H \mathbf{\Theta} \mathbf{A}_{rp} \mathbf{G}_p \mathbf{A}_b^H \mathbf{Q} \mathbf{A}_b \mathbf{G}_p^H \mathbf{A}_{rp}^H \mathbf{\Theta}^H \mathbf{A}_{rL} \mathbf{T}_L^H \mathbf{A}_u^H \mathbf{A}_u \right) \right] \\
&= \mathbb{E}_{\lambda} \left[\log_2 \prod_{i=1}^L \left(1 + \lambda_i \left(\frac{1}{\sigma^2} \mathbf{T}_L \mathbf{A}_{rL}^H \mathbf{\Theta} \mathbf{A}_{rp} \mathbf{G}_p \mathbf{A}_b^H \mathbf{Q} \mathbf{A}_b \mathbf{G}_p^H \mathbf{A}_{rp}^H \mathbf{\Theta}^H \mathbf{A}_{rL} \mathbf{T}_L^H \mathbf{A}_u^H \mathbf{A}_u \right) \right) \right]. \tag{55}
\end{aligned}$$

Then, when the SNR goes to infinity, we have

$$\begin{aligned}
C_h &= \mathbb{E}_\lambda \left[\log_2 \prod_{i=1}^L \lambda_i \left(\frac{1}{\sigma^2} \mathbf{T}_L \mathbf{A}_{rL}^H \Theta \mathbf{A}_{rp} \mathbf{G}_p \mathbf{A}_b^H \mathbf{Q} \mathbf{A}_b \mathbf{G}_p^H \mathbf{A}_{rp}^H \Theta^H \mathbf{A}_{rL} \mathbf{T}_L^H \mathbf{A}_u^H \mathbf{A}_u \right) \right] \\
&\stackrel{(a)}{\leq} \mathbb{E}_\lambda \left[\log_2 \prod_{i=1}^L \lambda_i \left(\frac{1}{\sigma^2} \mathbf{T}_L \mathbf{A}_{rL}^H \Theta \mathbf{A}_{rp} \mathbf{G}_p \mathbf{A}_b^H \mathbf{Q} \mathbf{A}_b \mathbf{G}_p^H \mathbf{A}_{rp}^H \Theta^H \mathbf{A}_{rL} \mathbf{T}_L^H \right) \lambda_i(\mathbf{A}_u^H \mathbf{A}_u) \right] \\
&\stackrel{(b)}{=} \mathbb{E}_\lambda \left[\log_2 \prod_{i=1}^L \lambda_i \left(\frac{1}{\sigma^2} \mathbf{A}_{rL}^H \Theta \mathbf{A}_{rp} \mathbf{G}_p \mathbf{A}_b^H \mathbf{Q} \mathbf{A}_b \mathbf{G}_p^H \mathbf{A}_{rp}^H \Theta^H \mathbf{A}_{rL} \mathbf{T}_L^H \mathbf{T}_L \right) \lambda_i(\mathbf{A}_u^H \mathbf{A}_u) \right],
\end{aligned} \tag{56}$$

where C_h denotes the ergodic capacity in the high-SNR regime, (a) holds due to Theorem in (40) and the equality holds when $N_s = P = L$, and (b) holds due to $\lambda(\mathbf{A}\mathbf{B}) = \lambda(\mathbf{B}\mathbf{A})$ for arbitrary matrices \mathbf{A} and \mathbf{B} . By repeatedly applying the theorem above, C_h in (56) can be expressed as

$$\begin{aligned}
C_h &\leq \mathbb{E}_\lambda \left[\log_2 \prod_{i=1}^L \lambda_i \left(\frac{1}{\sigma^2} \mathbf{A}_b^H \mathbf{Q} \mathbf{A}_b \right) \lambda_i(\mathbf{A}_u^H \mathbf{A}_u) \lambda_i(\mathbf{X}^H \mathbf{X}) \lambda_i(\mathbf{G}_p^H \mathbf{G}_p) \lambda_i(\mathbf{T}_L^H \mathbf{T}_L) \right] \\
&\stackrel{(a)}{=} \mathbb{E}_{g,t} \left[\log_2 \prod_{i=1}^L \frac{N_b N_u N_r^2}{\sigma^2 P L} d_{b,i} d_{u,i} d_{r,i} |g_i|^2 |t_i|^2 \right],
\end{aligned} \tag{57}$$

where $\mathbf{X} = \mathbf{A}_{rL}^H \Theta \mathbf{A}_{rp}$, (a) holds due to $\lambda_i \left(\frac{1}{\sigma^2} \mathbf{A}_b^H \mathbf{Q} \mathbf{A}_b \right) = \frac{1}{\sigma^2} d_{b,i}$, $\lambda_i(\mathbf{A}_u^H \mathbf{A}_u) = d_{u,i}$, $\lambda_i(\mathbf{X}^H \mathbf{X}) = d_{r,i}$, $\lambda_i(\mathbf{G}_p^H \mathbf{G}_p) = \frac{N_b N_r}{P} |g_i|^2$ and $\lambda_i(\mathbf{T}_L^H \mathbf{T}_L) = \frac{N_u N_r}{L} |t_i|^2$.

Since $g_i \sim \mathcal{CN}(0, 1)$, $t_i \sim \mathcal{CN}(0, 1)$, then $|g_i|^2 \sim \exp(1)$ and $|t_i|^2 \sim \exp(1)$. Let $\varrho_i = \frac{N_b N_u N_r^2}{\sigma^2 P L} d_{b,i} d_{u,i} d_{r,i}$, $x = |g_i|^2 |t_i|^2$ and $y = \log_2(\varrho_i x)$, the probability density function (PDF) $f_X(x)$ can be expressed as

$$f_X(x) = \int_0^\infty \frac{1}{z} e^{-(z+x/z)} dz, \quad x > 0. \tag{58}$$

The PDF $f_Y(y)$ can be expressed as

$$f_Y(y) = \frac{2^y \ln 2}{\varrho_i} \int_0^\infty \frac{1}{x} e^{-(x + \frac{2^y}{e_i x})} dx, \quad y > 0. \tag{59}$$

Therefore, we have

$$\begin{aligned}
C_h^{upper} &\triangleq \mathbb{E}_{g,t} \left[\log_2 \prod_{i=1}^{N_s} \frac{N_b N_u N_r^2}{\sigma^2 P L} d_{b,i} d_{u,i} d_{r,i} |g_i|^2 |t_i|^2 \right] \\
&= \sum_{i=1}^{N_s} \int_0^\infty \int_0^\infty \frac{\ln 2}{\varrho_i} 2^y y x^{-1} e^{-(x + \frac{2^y}{e_i x})} dx dy \\
&= \sum_{i=1}^{N_s} \frac{1}{\ln 2} \int_0^\infty e^{-x} [\psi(1) + \ln(\varrho_i x)] dx \\
&= \sum_{i=1}^{N_s} \frac{1}{\ln 2} [2\psi(1) + \ln(\varrho)],
\end{aligned} \tag{60}$$

where $\psi(x) = \frac{d}{dx} \ln \Gamma(x)$ is the Digamma function and $\psi(1) = -\gamma$.

D. Proof of Theorem 2

The ergodic capacity approximation C_{app} can be calculated as

$$\begin{aligned}
C_{app} &= \mathbb{E}_{g,t} \left[\sum_{i=1}^{N_s} \log_2 \left(1 + \frac{N_b N_u N_r^2}{\sigma^2 P L} d_{b,i} d_{u,i} d_{r,i} |g_i|^2 |t_i|^2 \right) \right] \\
&= \sum_{i=1}^{N_s} \int_0^\infty f_X(x) \log_2 \left(1 + \frac{N_b N_u N_r^2}{\sigma^2 P L} d_{b,i} d_{u,i} d_{r,i} x \right) dx \\
&= \frac{1}{\ln 2} \sum_{i=1}^{N_s} \int_0^\infty e^{-z} e^{\frac{1}{\alpha_i z}} E_1 \left(\frac{1}{\alpha_i z} \right) dz.
\end{aligned} \tag{61}$$

E. Proof of Theorem 3

If $c_i = 0$, we can add a very small real number $\delta > 0$, i.e., $c_i = \delta$. Then, we have

$$\begin{aligned}
\det [\mathbf{I} + \text{diag}(\mathbf{c}) \mathbf{U}^H \text{diag}(\mathbf{s}) \mathbf{U}] &= \det [\text{diag}(\mathbf{c}) (\text{diag}(\mathbf{c}^{-1}) + \mathbf{U}^H \text{diag}(\mathbf{s}) \mathbf{U})] \\
&= \det [\text{diag}(\mathbf{c}) (\mathbf{U} \text{diag}(\mathbf{c}^{-1}) \mathbf{U}^H + \text{diag}(\mathbf{s}))] \\
&\stackrel{(a)}{=} \det [\text{diag}(\mathbf{c})] \det [\mathbf{U} \text{diag}(\mathbf{c}^{-1}) \mathbf{U}^H + \text{diag}(\mathbf{s})],
\end{aligned} \tag{62}$$

where (a) holds due to $\det(\mathbf{AB}) = \det(\mathbf{A}) \det(\mathbf{B})$ for arbitrary matrices \mathbf{A} and \mathbf{B} .

According to [[29], 9.G.3], if \mathbf{G} and \mathbf{H} are $n \times n$ Hermitian matrices, then

$$\det(\mathbf{G} + \mathbf{H}) = \prod_{i=1}^n \lambda_i(\mathbf{G} + \mathbf{H}) \leq \prod_{i=1}^n [\lambda_i(\mathbf{G}) + \lambda_{n-i+1}(\mathbf{H})], \tag{63}$$

where $\lambda_i(\cdot)$ denotes the i -th largest eigenvalue of the input matrix. Thus, we have

$$\begin{aligned}
\det [\mathbf{U} \text{diag}(\mathbf{c}^{-1}) \mathbf{U}^H + \text{diag}(\mathbf{s})] &= \prod_{i=1}^N \lambda_i (\mathbf{U} \text{diag}(\mathbf{c}^{-1}) \mathbf{U}^H + \text{diag}(\mathbf{s})) \\
&\stackrel{(a)}{\leq} \prod_{i=1}^N [\lambda_i(\mathbf{U} \text{diag}(\mathbf{c}^{-1}) \mathbf{U}^H) + \lambda_{N-i+1}(\text{diag}(\mathbf{s}))] \\
&\stackrel{(b)}{=} \prod_{i=1}^N [\lambda_i(\text{diag}(\mathbf{c}^{-1})) + \lambda_{N-i+1}(\text{diag}(\mathbf{s}))] \\
&\stackrel{(c)}{=} \prod_{i=1}^N (c_{N-i+1}^{-1} + s_{N-i+1}),
\end{aligned} \tag{64}$$

where (a) holds due to the Theorem [[29], 9.G.3], (b) holds due to $\lambda(\mathbf{AB}) = \lambda(\mathbf{BA})$ for arbitrary matrices \mathbf{A} and \mathbf{B} , and (c) holds due to the fact that \mathbf{c} and \mathbf{s} are the descending ordered sequences.

As a result, we have

$$\begin{aligned}
 \det [\mathbf{I} + \text{diag}(\mathbf{c})\mathbf{U}^H \text{diag}(\mathbf{s})\mathbf{U}] &= \det [\text{diag}(\mathbf{c})] \det [\mathbf{U} \text{diag}(\mathbf{c}^{-1})\mathbf{U}^H + \text{diag}(\mathbf{s})] \\
 &\leq \prod_{i=1}^N c_i \prod_{i=1}^N (c_i^{-1} + s_i) \\
 &= \prod_{i=1}^N (1 + c_i s_i) \\
 &= \det [\mathbf{I} + \mathbf{U}^H \text{diag}(\mathbf{c}) \text{diag}(\mathbf{s})\mathbf{U}].
 \end{aligned} \tag{65}$$

REFERENCES

- [1] A. Ghosh, T. A. Thomas, M. C. Cudak, R. Ratasuk, P. Moorut, F. W. Vook, T. S. Rappaport, G. R. MacCartney, S. Sun, and S. Nie, "Millimeter-wave enhanced local area systems: A high-data-rate approach for future wireless networks," *IEEE J. Sel. Areas Commun.*, vol. 32, no. 6, pp. 1152–1163, 2014.
- [2] Y. Niu, Y. Li, D. Jin, L. Su, and A. V. Vasilakos, "A survey of millimeter wave communications (mmwave) for 5G: opportunities and challenges," *Wireless networks*, vol. 21, no. 8, pp. 2657–2676, 2015.
- [3] G. R. MacCartney, T. S. Rappaport, and S. Rangan, "Rapid fading due to human blockage in pedestrian crowds at 5G millimeter-wave frequencies," in *IEEE Proc. of Global Commun. Conf. (GLOBECOM)*, 2017, pp. 1–7.
- [4] Q. Wu and R. Zhang, "Towards smart and reconfigurable environment: Intelligent reflecting surface aided wireless network," *IEEE Commun. Mag.*, vol. 58, no. 1, pp. 106–112, 2020.
- [5] N. S. Perovic, M. D. Renzo, and M. F. Flanagan, "Channel capacity optimization using reconfigurable intelligent surfaces in indoor mmWave environments," in *IEEE Proc. of International Commun. Conf. (ICC)*, 2020, pp. 1–7.
- [6] E. Basar, M. Di Renzo, J. De Rosny, M. Debbah, M.-S. Alouini, and R. Zhang, "Wireless communications through reconfigurable intelligent surfaces," *IEEE Access*, vol. 7, pp. 116 753–116 773, 2019.
- [7] Q. Wu and R. Zhang, "Intelligent reflecting surface enhanced wireless network via joint active and passive beamforming," *IEEE Trans. Wireless Commun.*, vol. 18, no. 11, pp. 5394–5409, 2019.
- [8] H. Guo, Y.-C. Liang, J. Chen, and E. G. Larsson, "Weighted sum-rate maximization for reconfigurable intelligent surface aided wireless networks," *IEEE Trans. Wireless Commun.*, vol. 19, no. 5, pp. 3064–3076, 2020.
- [9] M. Cui, G. Zhang, and R. Zhang, "Secure wireless communication via intelligent reflecting surface," *IEEE Wireless Commun. Lett.*, vol. 8, no. 5, pp. 1410–1414, 2019.
- [10] S. Zhang and R. Zhang, "Capacity characterization for intelligent reflecting surface aided MIMO communication," *IEEE J. Sel. Areas Commun.*, vol. 38, no. 8, pp. 1823–1838, 2020.
- [11] P. Wang, J. Fang, L. Dai, and H. Li, "Joint transceiver and large intelligent surface design for massive MIMO mmwave systems," *IEEE Trans. Wireless Commun.*, vol. 20, no. 2, pp. 1052–1064, 2021.
- [12] T. Van Chien, L. T. Tu, S. Chatzinotas, and B. Ottersten, "Coverage probability and ergodic capacity of intelligent reflecting surface-enhanced communication systems," *IEEE Commun. Lett.*, vol. 25, no. 1, pp. 69–73, 2021.

- [13] C. Singh and C. H. Lin, "Reconfigurable intelligent surfaces aided communication: Capacity and performance analysis over rician fading channel," *arXiv preprint arXiv:2107.10937*, 2021. [Online]. Available: <https://arxiv.org/abs/2107.10937>
- [14] Y. Han, W. Tang, S. Jin, C.-K. Wen, and X. Ma, "Large intelligent surface-assisted wireless communication exploiting statistical CSI," *IEEE Trans. Veh. Technol.*, vol. 68, no. 8, pp. 8238–8242, 2019.
- [15] X. Hu, J. Wang, and C. Zhong, "Statistical CSI based design for intelligent reflecting surface assisted MISO systems," *Sci. China Inf. Sci.*, vol. 63, no. 12, pp. 1–10, 2020.
- [16] K. Zhi, C. Pan, H. Ren, and K. Wang, "Power scaling law analysis and phase shift optimization of ris-aided massive MIMO systems with statistical CSI," 2021. [Online]. Available: <https://arxiv.org/abs/2010.13525>
- [17] J. Wang, H. Wang, Y. Han, S. Jin, and X. Li, "Joint transmit beamforming and phase shift design for reconfigurable intelligent surface assisted MIMO systems," *IEEE Trans. on Cogn. Commun. Netw.*, vol. 7, no. 2, pp. 354–368, 2021.
- [18] J. Zhang, J. Liu, S. Ma, C.-K. Wen, and S. Jin, "Large system achievable rate analysis of RIS-assisted MIMO wireless communication with statistical CSIT," *IEEE Trans. Wireless Commun.*, vol. 20, no. 9, pp. 5572–5585, 2021.
- [19] C. Ouyang, S. Wu, C. Jiang, Y. Liu, and H. Yang, "On the ergodic capacity of reconfigurable intelligent surface (RIS)-aided MIMO channels," 2021. [Online]. Available: <https://arxiv.org/abs/2106.10444>
- [20] A. Alkhateeb, O. El Ayach, G. Leus, and R. W. Heath, "Channel estimation and hybrid precoding for millimeter wave cellular systems," *IEEE J. Sel. Topics Signal Process.*, vol. 8, no. 5, pp. 831–846, 2014.
- [21] O. E. Ayach, S. Rajagopal, S. Abu-Surra, Z. Pi, and R. W. Heath, "Spatially sparse precoding in millimeter wave MIMO systems," *IEEE Trans. Wireless Commun.*, vol. 13, no. 3, pp. 1499–1513, 2014.
- [22] X. Yu, J.-C. Shen, J. Zhang, and K. B. Letaief, "Alternating minimization algorithms for hybrid precoding in millimeter wave MIMO systems," *IEEE J. Sel. Topics Signal Process.*, vol. 10, no. 3, pp. 485–500, 2016.
- [23] S. Sun and T. S. Rappaport, "Millimeter wave MIMO channel estimation based on adaptive compressed sensing," in *IEEE Int. Conf. Commun. Workshops (ICCW)*, 2017, pp. 47–53.
- [24] X. Yang, X. Li, S. Zhang, and S. Jin, "On the ergodic capacity of mmwave systems under finite-dimensional channels," *IEEE Trans. Wireless Commun.*, vol. 18, no. 11, pp. 5440–5453, 2019.
- [25] F. Shu, Y. Chen, X. You, and J. Lu, "Low-complexity optimal spatial channel pairing for AF-based multi-pair two-way relay networks," *Sci. China Inf. Sci.*, vol. 57, no. 10, pp. 1–10, 2014.
- [26] H. N. Nagaraja, "Order statistics from independent exponential random variables and the sum of the top order statistics," in *Advances in Distribution Theory, Order Statistics, and Inference*. Springer, 2006, pp. 173–185.
- [27] X. Yu, D. Xu, and R. Schober, "MISO wireless communication systems via intelligent reflecting surfaces," in *Proc. IEEE/CIC Int. Conf. Commun. China (ICCC)*, 2019, pp. 735–740.
- [28] P.-A. Absil, R. Mahony, and R. Sepulchre, *Optimization Algorithms on Matrix Manifolds*. Princeton University Press, 2009. [Online]. Available: <https://doi.org/10.1515/9781400830244>
- [29] A. W. Marshall, I. Olkin, and B. C. Arnold, *Inequalities: theory of majorization and its applications*. Springer, 1979, vol. 143.
- [30] X. Zhan, *Matrix inequalities*. Springer, 2004, vol. 1790.